1 The Physical Basis of NMR Spectroscopy

1.1 Introduction

In 1946 two research groups, that of F. Bloch, W.W. Hansen and M. E. Packard and that of E. M. Purcell, H. C. Torrey and R.V. Pound, independently observed nuclear magnetic resonance signals for the first time. Bloch and Purcell were jointly awarded the Nobel Prize for Physics in 1952 for their discovery. Since then nuclear magnetic resonance (NMR) spectroscopy has developed into an indispensable tool for chemists, biochemists, physicists, and more recently medical scientists. During the first three decades of NMR spectroscopy all measurements relied on *one-dimensional* modes of observation; this gives spectra having just *one* frequency axis, the second axis being used to display the signal intensities. The development of *two-dimensional* NMR experiments during the 1970s heralded the start of a new era in NMR spectroscopy. Spectra recorded by these methods have *two* frequency axes, the intensities being displayed in the third dimension. More recently it has even become possible to perform experiments with three or more dimensions, although these are still far from being routine techniques. The importance of the position that NMR spectroscopy now occupies is illustrated by the awards of the Nobel Prize for Chemistry in 1991 to R.- R. Ernst and in 2002 to K. Wüthrich, and of the Nobel Prize for Medicine in 2003 to P. Lauterbur and P. Mansfield for their pioneering research on NMR methods in chemistry, biochemistry and medicine. The new techniques that have emerged during the last few years show that developments in NMR spectroscopy are still far from coming to an end.

This book aims to explain why it is that, for chemists especially, NMR spectroscopy has become (possibly) the most important of all spectroscopic methods.

The main field of application of NMR spectroscopy is that of determining the structures of molecules. The necessary information for this is obtained by measuring, analyzing and interpreting high-resolution NMR spectra recorded on liquids of low viscosity (or in some cases on solids by using special techniques and instruments that have been developed in the last few years). In this book we will confine our attention almost exclu-

Basic One- and Two-Dimensional Spectroscopy. 5th Edition. Horst Friebolin

ISBN 978-3-527-32782-9

sively to *high-resolution* NMR spectroscopy on liquids, since solid-state measurements involve quite different experimental techniques and the interpretation often brings in extra complications.

The nuclides that mainly interest us are protons (^{1}H) and carbon-13 (^{13}C), as their resonances are the most important ones for determining the structures of organic molecules. However, in the following chapters we shall meet also examples of NMR spectroscopy of other nuclides whose NMR signals can now be observed without difficulty.

In order to understand NMR spectroscopy we first need to learn how nuclei which have a nuclear angular momentum $\boldsymbol{P}$ and a magnetic moment $\boldsymbol{\mu}$ behave in a static magnetic field. Following this we shall discuss the basic NMR experiment, the different methods of observation, and the spectral parameters.

1.2 Nuclear Angular Momentum and Magnetic Moment

Most nuclei possess a nuclear or intrinsic angular momentum $\boldsymbol{P}$. According to the classical picture the atomic nucleus, assumed to be spherical, rotates about an axis. Quantum mechanical considerations show that, like many other atomic quantities, this angular momentum is quantized:

$$P = \sqrt{I(I+1)}\,\hbar \qquad (1\text{-}1)$$

Here $\hbar = h/2\pi$, where h is Planck's constant (= 6.6256 x 10^{-34} J s), and I is the angular momentum quantum number, usually called simply the nuclear spin. The nuclear spin can have the values $I = 0, 1/2, 1, 3/2, 2 \ldots$ up to 6 (see also Table 1-1). Neither the values of I nor those of P can yet be predicted from theory.

The angular momentum $\boldsymbol{P}$ has associated with it a magnetic moment $\boldsymbol{\mu}$. Both are vector quantities, and they are proportional to each other:

$$\boldsymbol{\mu} = \gamma \boldsymbol{P} \qquad (1\text{-}2)$$

The proportionality factor γ is a constant for each nuclide (i. e. each isotope of each element), and is called the magnetogyric ratio. The detection sensitivity of a nuclide in the NMR experiment depends on γ; nuclides with a large value of γ are said to be sensitive (i. e. easy to observe), while those with a small γ are said to be insensitive.

By combining Equations (1-1) and (1-2) we obtain for the magnetic moment μ:

$$\mu = \gamma \sqrt{I(I+1)}\,\hbar \qquad (1\text{-}3)$$

Table 1-1.
Properties of some nuclides of importance in NMR spectroscopy.

Nuclide	Spin I	Natural abundance[a] [%]	Magnetic Moment[b] μ_z/μ_N	Electric quadrupole moment[a] Q [10^{-30} m^2]	Magnetogyric ratio[a] γ [10^7 rad T^{-1} s^{-1}]	NMR frequency[a] [MHz] (B_0 = 2.3488 T)	Relative receptivity[c]
^{1}H	1/2	99.9885	2.7928	–	26.7522	100.000	1.00
^{2}H	1	0.0115	0.8574	0.2860	4.1066	15.3506	9.65 x 10^{-3}
^{3}H[d]	1/2	–	2.9790	–	28.5350	106.6640	1.21
^{6}Li	1	7.59	0.8220	–0.0808	3.9372	14.7170	8.50 x 10^{-3}
^{10}B	3	19.9	1.8006	8.459	2.8747	10.7456	1.99 x 10^{-2}
^{11}B	3/2	80.1	2.6887	4.059	8.5847	32.0897	1.65 x 10^{-1}
^{12}C	0	98.9	–	–	–	–	–
^{13}C	1/2	1.07	0.7024	–	6.7283	25.1504	1.59 x 10^{-2}
^{14}N	1	99.63	0.4038	2.044	1.9338	7.2285	1.01 x 10^{-3}
^{15}N	1/2	0.368	–0.2832	–	–2.7126	10.1398	1.04 x 10^{-3}
^{16}O	0	99.96	–	–	–	–	–
^{17}O	5/2	0.038	–1.8938	–2.558	–3.6281	13.5617	2.91 x 10^{-2}
^{19}F	1/2	100	2.6269	–	25.1815	94.0670	8.32 x 10^{-1}
^{23}Na	3/2	100	2.2177	10.4	7.0809	26.4683	9.27 x 10^{-2}
^{25}Mg	5/2	10.00	–0.8555	19.94	–1.6389	6.1260	2.68 x 10^{-3}
^{29}Si	1/2	4.68	–0.5553	–	–5.3190	19.8826	7.86 x 10^{-3}
^{31}P	1/2	100	1.1316	–	10.8394	40.5178	6.65 x 10^{-2}
^{39}K	3/2	93.258	0.3915	5.85	1.2501	4.6727	5.10 x 10^{-4}
^{43}Ca	7/2	0.135	–1.3176	–4.08	–1.8031	6.7399	6.43 x 10^{-3}
^{57}Fe	1/2	2.119	0.0906	–	0.8681	3.2448	3.42 x 10^{-5}
^{59}Co	7/2	100	4.627	42.0	6.332	23.6676	2.78 x 10^{-1}
^{119}Sn	1/2	8.59	–1.0473	–	–10.0317	37.2906	5.27 x 10^{-2}
^{133}Cs	7/2	100	2.5820	–0.343	3.5333	13.1161	4.84 x 10^{-2}
^{195}Pt	1/2	33.832	0.6095	–	5.8385	21.4968	1.04 x 10^{-2}

[a] Values from [1].
[b] z-component of nuclear magnetic moment in units of the nuclear magneton μ_N.
Values from the Bruker Almanac 2010. $\mu_N = eh/4\pi m_p$, m_p: mass of the proton = 5.05095 x 10^{-27} JT^{-1}.
[c] Receptivity is expressed relative to ^{1}H (= 1) for constant field and equal numbers of nuclei.
Values from the Bruker Almanac 2010.
[d] ^{3}H is radioactive.

Nuclides with spin $I = 0$ therefore have no nuclear magnetic moment. Two very important facts for our purposes are that the ^{12}C isotope of carbon and the ^{16}O isotope of oxygen belong to this class of nuclides – this means that the main building blocks of organic compounds cannot be observed by NMR spectroscopy.

For most nuclides the nuclear angular momentum vector $\boldsymbol{P}$ and the magnetic moment vector $\boldsymbol{\mu}$ point in the same direction, i. e. they are parallel. However, in a few cases, for example ^{15}N and ^{29}Si (and also the electron!), they are antiparallel. The consequences of this will be considered in Chapter 10.

1.3 Nuclei in a Static Magnetic Field

1.3.1 Directional Quantization

If a nucleus with angular momentum $\boldsymbol{P}$ and magnetic moment $\boldsymbol{\mu}$ is placed in a static magnetic field $\boldsymbol{B}_0$, the angular momentum takes up an orientation such that its component P_z along the direction of the field is an integral or half-integral multiple of $\hbar$:

$$P_z = m\,\hbar \tag{1-4}$$

Here m is the magnetic or directional quantum number, and can take any of the values $m = I, I-1, \ldots\ldots -I$.

It can easily be deduced that there are $(2I + 1)$ different values of m, and consequently an equal number of possible orientations of the angular momentum and magnetic moment in the magnetic field. This behavior of the nuclei in the magnetic field is called *directional quantization*. For protons and ^{13}C nuclei, which have $I = 1/2$, this results in two m-values (+ 1/2 and −1/2); however, for nuclei with $I = 1$, such as ^{2}H and ^{14}N, there are three values ($m = +1, 0$ and -1; see Fig. 1-1).

From Equations (1-2) and (1-4) we obtain the components of the magnetic moment along the field direction z:

$$\mu_z = m\,\gamma\,\hbar \tag{1-5}$$

In the classical representation the nuclear dipoles precess around the z-axis, which is the direction of the magnetic field – their behavior resembles that of a spinning top (Fig. 1-2). The precession frequency or Larmor frequency ν_L is proportional to the magnetic flux density B_0:

$$\nu_L = \left|\frac{\gamma}{2\pi}\right| B_0 \tag{1-6}$$

However, in contrast to the classical spinning top, for a precessing nuclear dipole only certain angles are allowed, because of the directional quantization. For the proton with $I = 1/2$, for example, this angle is 54° 44′.

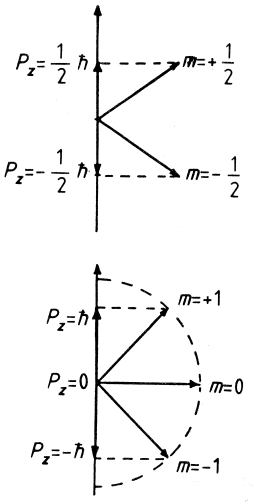

Figure 1-1.
Directional quantization of the angular momentum $\boldsymbol{P}$ in the magnetic field for nuclei with $I = 1/2$ and 1.

1.3.2 Energy of the Nuclei in the Magnetic Field

The energy of a magnetic dipole in a magnetic field with a flux density B_0 is:

$$E = -\mu_z\,B_0 \tag{1-7}$$

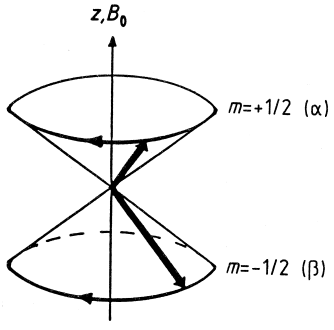

Figure 1-2.
Precession of nuclear dipoles with spin $I = 1/2$ around a double cone; the half-angle of the cone is 54°44′.

Thus, for a nucleus with $(2I + 1)$ possible orientations there are also $(2I + 1)$ energy states, which are called the nuclear Zeeman levels. From Equation (1-5) we have:

$$E = -m\gamma\hbar B_0 \tag{1-8}$$

For the proton and the ^{13}C nucleus, both of which have $I = 1/2$, there are two energy values in the magnetic field corresponding to the two m-values $+ 1/2$ and $- 1/2$. If $m = + 1/2$, μ_z is parallel to the field direction, which is the energetically preferred orientation; conversely, for $m = - 1/2$, μ_z is antiparallel. In quantum mechanics the $m = + 1/2$ state is described by the spin function α, while the $m = - 1/2$ state is described by the spin function β; the exact form of these functions need not concern us here.

For nuclei with $I = 1$, such as ^2H and ^{14}N, there are three m-values $(+1, 0$ and $-1)$ and therefore three energy levels (Fig. 1-3).

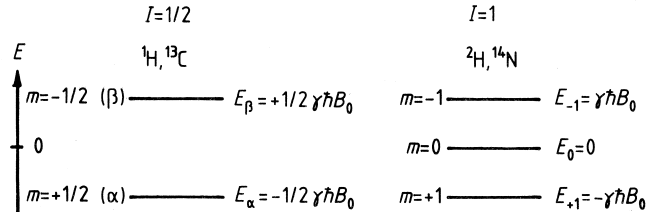

Figure 1-3.
Energy level schemes for nuclei with $I = 1/2$ (left) and $I = 1$ (right).

The energy difference between two adjacent energy levels is:

$$\Delta E = \gamma\hbar B_0 \tag{1-9}$$

Figure 1-4 illustrates, taking the example of nuclei with $I = 1/2$, that ΔE is proportional to B_0.

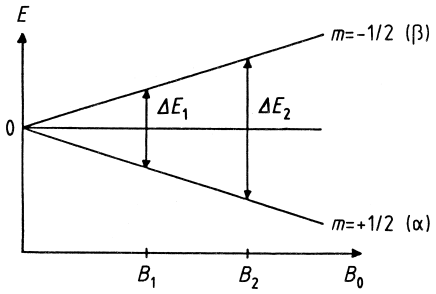

Figure 1-4.
The energy difference ΔE between two adjacent energy levels as a function of the magnetic flux density B_0.

1.3.3 Populations of the Energy Levels

How do the nuclei in a macroscopic sample, such as that in an NMR sample tube, distribute themselves between the different energy states in thermal equilibrium? The answer to this question is provided by Boltzmann statistics. For nuclei with $I = 1/2$, if we represent the number of nuclei in the upper energy level by N_β and the number in the lower energy level by N_α, then:

$$\frac{N_\beta}{N_\alpha} = e^{-\Delta E/k_B T} \approx 1 - \frac{\Delta E}{k_B T} = 1 - \frac{\gamma \hbar B_0}{k_B T} \qquad (1\text{-}10)$$

where k_B is the Boltzmann constant ($= 1.3805 \times 10^{-23}$ J K^{-1}) and T is the absolute temperature in K.

For protons – and also for all other nuclides – the energy difference ΔE is very small compared with the average energy $k_B T$ of the thermal motions, and consequently the populations of the energy levels are nearly equal. The excess in the lower energy level is only in the region of parts per million (ppm).

Numerical example for protons:

○ With a magnetic flux density $B_0 = 1.41$ T (resonance frequency 60 MHz) the energy difference is given by Equation (1-9) as:
$\Delta E \approx 2.4 \times 10^{-2}$ J mol^{-1} ($\approx 0.6 \times 10^{-2}$ cal mol^{-1}).
The γ-value needed for the calculation can be obtained from Table 1-1; alternatively we can anticipate Section 1.4.1 and calculate it from Equation (1-12).
For a temperature of 300 K these values give:
$N_\beta \approx 0.9999904\ N_\alpha$.
For $B_0 = 7.05$ T (resonance frequency 300 MHz) the difference is greater:
$N_\beta \approx 0.99995\ N_\alpha$.

1.3.4 Macroscopic Magnetization

According to the classical picture, a nucleus with $I = 1/2$ (e. g. ^{1}H or ^{13}C) precesses around the field axis z on the surface of a double cone as shown in Figure 1-5. If we add the z-components of all the nuclear magnetic moments in a sample we obtain a macroscopic magnetization $\boldsymbol{M}_0$ along the field direction, since N_α is greater than N_β. The vector $\boldsymbol{M}_0$ plays an important role in the description of all types of pulsed NMR experiments.

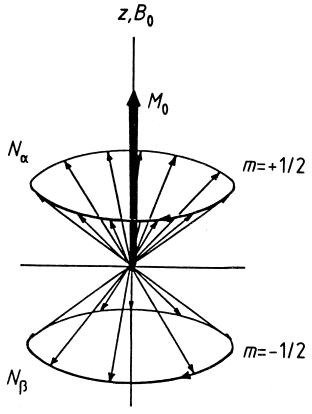

Figure 1-5.
Distribution of the precessing nuclear dipoles (total number $N = N_\alpha + N_\beta$) around the double cone. As $N_\alpha > N_\beta$ there is a resultant macroscopic magnetization $\boldsymbol{M}_0$.

1.4 Basic Principles of the NMR Experiment

1.4.1 The Resonance Condition

In the nuclear magnetic resonance experiment transitions are induced between different energy levels by irradiating the nuclei with a superimposed field B_1 of the correct quantum energy, i. e. with electromagnetic waves of the appropriate frequency ν_1. This condition enables the magnetic component of the radiation to interact with the nuclear dipoles.

Let us consider the protons in a solution of chloroform ($CHCl_3$). The energy level scheme on the left-hand side of Figure 1-3 is appropriate for this case, and transitions between the energy levels can occur when the frequency ν_1 is chosen so that Equation (1-11) is satisfied:

$$h\,\nu_1 = \Delta E \tag{1-11}$$

Transitions from the lower to the upper energy level correspond to an absorption of energy, and those in the reverse direction to an emission of energy (arrows labeled 'a' and 'e' respectively in Figure 1-6). Both transitions are possible, and they are equally probable. Each transition is associated with a reversal of the spin orientation. Due to the population excess in the lower level, the absorption of energy from the irradiating field is the dominant process. This is observed as a signal, whose intensity is proportional to the population difference N_α-N_β, and is therefore also proportional to the total number of spins in the sample, and thus to the concentration. However, if the populations are equal ($N_\alpha = N_\beta$) the absorption and emission processes cancel each other and no signal is observed. This condition is called *saturation*.

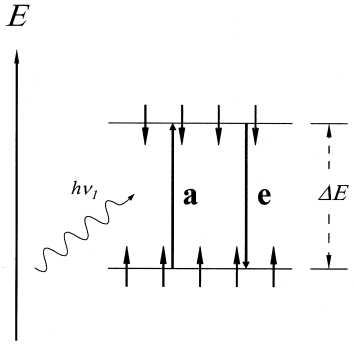

Figure 1-6.
Energy level scheme for a system of nuclei with spin $I = 1/2$. Irradiation with the frequency ν_1 such that $h\nu_1 = \Delta E$ induces absorption (a) and emission (e) transitions.

From Equations (1-9) and (1-11) we obtain the *resonance condition:*

$$\nu_L = \nu_1 = \left|\frac{\gamma}{2\pi}\right| B_0 \tag{1-12}$$

The term "resonance" relates to the classical interpretation of the phenomenon, since transitions only occur when the frequency ν_1 of the electromagnetic radiation matches the Larmor frequency ν_L.

So far we have considered nuclei with $I = 1/2$, for which there are only two energy levels. But what transitions are allowed when there are more than two such levels, as is the case for nuclei with $I \geqslant 1$ (Fig. 1-3, right-hand level scheme), and for the coupled systems with several nuclei which will be discussed

later? The answer provided by quantum mechanics is that only those transitions in which the magnetic quantum number m changes by 1, i. e. single quantum transitions, are allowed:

$$\Delta m = \pm 1 \tag{1-13}$$

Therefore the only transitions that can take place are those between adjacent energy levels. According to this selection rule the transition from $m = +1$ to $m = -1$ for a ^{14}N nucleus is forbidden.

Although coupled spin systems will not be treated until later, we shall point out here that a simultaneous flipping of two or more spins is forbidden. For example, in a two-spin system one could imagine, in addition to the single-quantum transitions, two other possible transitions, whereby both nuclei are initially in the α-state ($m = +1/2$) and simultaneously change to the β-state ($m = -1/2$). This would be a double quantum transition, since the sum of the magnetic quantum numbers changes by two ($\Delta m = 2$). Or again we could have one nucleus switching from the α- to the β-state while simultaneously the other switches from the β- to the α-state. In this case $\Delta m = 0$, i. e. we would have a zero-quantum transition. According to Equation (1-13) such double-quantum and zero-quantum transitions are forbidden.

1.4.2 Basic Principle of the NMR Measurement

NMR transitions in an analytical sample, producing a signal in the receiver channel of the spectrometer, occur when the resonance condition (Eq. 1-12) is satisfied. The most obvious and straightforward way to arrive at this condition and to record a spectrum is either to vary the magnetic flux density B_0 with a constant transmitter frequency ν_1 (field sweep method), or to vary the transmitter frequency ν_1 with constant flux density B_0 (frequency sweep method). In either case the recorder drive is linked directly to the field or frequency sweep, so that the recorder pen progressively traces out the spectrum. This is called the continuous wave (CW) method, as it uses uninterrupted radiofrequency power, unlike the pulsed method described in the next section. The CW method was the basis of all NMR spectrometers constructed up to about the end of the 1960s, but it has been entirely superseded by the pulsed method, for reasons that we shall see later.

The CW method was usually adequate for recording the spectra of sensitive nuclides such as ^1H, ^{19}F and ^{31}P; these have $I = 1/2$ with large magnetic moments, and also high natural

abundance. Routine measurements on insensitive nuclides and those with low natural abundance, ^{13}C for example, and also on very dilute solutions, were at first out of the question. To make this possible it was necessary to develop new NMR spectrometers and new measurement techniques.

With regard to spectrometers an important innovation was the introduction of cryomagnets, which make possible considerably higher magnetic field strengths ($B_0 > 2.35$ T) than can be reached with permanent magnets or electromagnets (see Table 1-2), and therefore higher sensitivities. However, the decisive step forward was achieved through *pulsed NMR spectroscopy*, a technique whose development has been closely linked to the rapid advances made in computer technology. During the 1960s R.-R. Ernst, together with W.-A. Anderson [2], pioneered the application of such techniques to NMR spectroscopy (pulsed Fourier transform or PFT spectroscopy), and thereby initiated the development of a new generation of spectrometers and experiments (see Chapters 8 and 9). The text of Ernst's Nobel Lecture [3] gives a fascinating insight into this phase of the development of NMR spectroscopy. The pulsed Fourier transform method will be described in detail in the next section, as it forms the basis of modern NMR spectroscopy.

The treatment given here will be based on the classical description using vector diagrams, as already introduced in Section 1.3. Then, in Section 1.5.6, we will come to the basic principles and main features of an NMR spectrometer.

Table 1-2.
^1H and ^{13}C resonance frequencies at different magnetic flux densities B_0.[a)]

B_0 [T]	Resonance frequencies [MHz]	
	^1H	^{13}C
2.35	100	25.15
4.70	200	50.32
5.87	250	62.90
7.05	300	75.47
9.40	400	100.61
11.75	500	125.76
14.10	600	150.90
16.44	700	176.05
17.62	750	188.62
18.79	800	201.19
21.14	900	226.34
23.49	1000	251.48

[a)] Values from the Bruker Almanac 2010.

1.5 The Pulsed NMR Method

1.5.1 The Pulse

In the pulse method all the nuclei of one species in the sample, e. g. all the protons or all the ^{13}C nuclei, are excited *simultaneously* by a radiofrequency pulse. What does such a pulse consist of, and how is it generated?

A radiofrequency generator usually operates at a fixed frequency ν_1. However, if it is switched on only for a short time τ_P, one obtains a pulse which contains not just the frequency ν_1 but a continuous band of frequencies symmetrical about the center frequency ν_1. However, only a part of the frequency band is effective in exciting transitions, and this part is approximately proportional to τ_P^{-1}. In NMR experiments the *pulse duration* τ_P is of the order of a few μs (Fig. 1-7).

The choice of the generator frequency ν_1 is determined by B_0 and the nuclide to be observed. For example, to observe proton

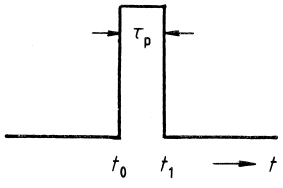

Figure 1-7.
Schematic representation of a pulse. The r. f. generator (frequency ν_1) is switched on at time t_0 and off at t_1. The pulse duration τ_P is typically several μs.

transitions at $B_0 = 4.70$ T, the required generator frequency is 200 MHz, whereas for observing ^{13}C resonances it must be 50.32 MHz. The pulse duration needed for the experiment depends on the width of the spectrum. For example, if $\tau_P = 10^{-5}$ s the frequency band is about 10^5 Hz wide. Provided that ν_1 is correctly chosen, all the frequencies in the spectrum to be recorded are contained in this band (Fig. 1-8).

The amplitudes of the frequency components of a pulse decrease with increasing separation from ν_1. Since, however, it is desirable that all the nuclei should be irradiated equally in the experiment so far as possible (see Section 1.6.3), "hard pulses" are used, i. e. short pulses of high power. The pulse duration is so chosen that the frequency band width exceeds the width of the spectrum by one to two powers of ten; the power level is typically several watts.

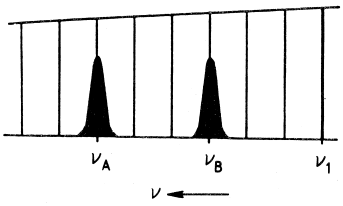

Figure 1-8.
Frequency components of a pulse. The band extends approximately from $\nu_1 - \tau_P^{-1}$ to $\nu_1 + \tau_P^{-1}$; ν_1 is the generator frequency and ν_A and ν_B are the resonance frequencies of nuclei A and B.

1.5.2 The Pulse Angle

We consider the simplest case, that of a sample containing only one nuclear species *i*, for example the protons in a chloroform solution ($CHCl_3$). As shown in Figure 1-5, the nuclear moments precess with the Larmor frequency ν_L on the surface of a double cone, and as a result of the difference in populations there is a macroscopic magnetization $\boldsymbol{M}_0$ along the field direction. To induce NMR transitions the radiofrequency pulse is applied to the sample along the direction of the *x*-axis. The magnetic vector of this electromagnetic radiation is then able to interact with the nuclear dipoles, and therefore with $\boldsymbol{M}_0$. So that we can more easily visualize this quantum mechanical process, the linear alternating magnetic field along the *x*-direction will be represented by two vectors with the same magnitude B_1, rotating in the *x*, *y*-plane with the same frequency ν_L, one of which, $\boldsymbol{B}_1$ (r), rotates clockwise, while the other, $\boldsymbol{B}_1$ (l), rotates anticlockwise (Fig. 1-9). The sum of these two vectors gives the alternating magnetic field along the *x*-direction, its maximum value being $2B_1$. Of the two rotating magnetic field components only the one which has the same direction of rotation as the precessing nuclear dipoles can interact with them (and thus with $\boldsymbol{M}_0$); from now on this component will be called simply $\boldsymbol{B}_1$. Under its influence $\boldsymbol{M}_0$ is tipped away from the *z*-axis (the direction of the static field $\boldsymbol{B}_0$); this tilting occurs in a plane perpendicular to the direction of $\boldsymbol{B}_1$. However, as this plane rotates with the Larmor frequency ν_L, the complicated motion of $\boldsymbol{M}_0$ is difficult to show in a diagram. If instead of the fixed coordinate system *x, y, z* we use a *rotating coordinate system x′, y′, z,* which rotates with the same frequency as $\boldsymbol{B}_1$, the

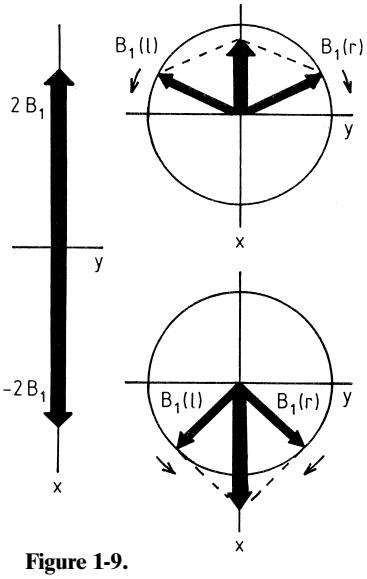

Figure 1-9.
Representation of a linear alternating field (max. $2B_1$) as the sum of two rotating fields, B_1 (r) (clockwise) and B_1 (l) (anticlockwise).

orientation and magnitude of $\boldsymbol{B}_1$ in this system are fixed. As the x'-axis of the rotating coordinate system is normally defined as being along the direction of $\boldsymbol{B}_1$, the effect of $\boldsymbol{B}_1$ is to turn the vector $\boldsymbol{M}_0$ about the x'-axis, i. e. in the y', z-plane. Equation (1-14) shows that the angle Θ through which it is tipped increases with the amplitude B_{1i} of the component of the r. f. pulse at the frequency ν_i of the nuclear resonance transition, and with the length of time for which the pulse is applied.

$$\Theta = \gamma B_{1i} \tau_P \tag{1-14}$$

The angle Θ is called the *pulse angle*. The majority of pulse techniques can be understood in terms of two special cases, namely experiments with pulse angles of 90° and 180°. If, as in the case just described, the direction of $\boldsymbol{B}_1$ coincides with that of the x'-axis, these are called $90^\circ_{x'}$ and $180^\circ_{x'}$ pulses. In Figure 1-10 the position of the magnetization vector following a $90^\circ_{x'}$ pulse, a $180^\circ_{x'}$ pulse, and a pulse of arbitrary angle $\Theta_{x'}$ is shown. In the vector diagrams the direction of $\boldsymbol{B}_1$ is indicated by a wavy line.

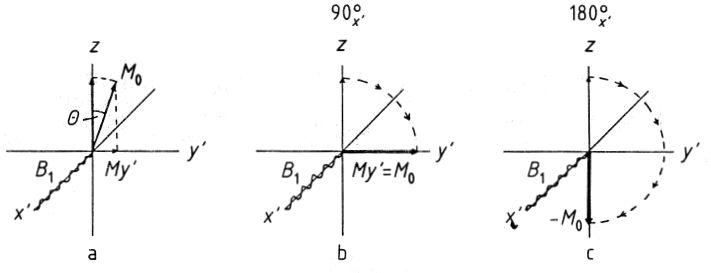

Figure 1-10.
Direction of the macroscopic magnetization vector $\boldsymbol{M}_0$ in the rotating coordinate system:
a) after a pulse of arbitrary angle $\Theta_{x'}$; b) after a $90^\circ_{x'}$ pulse; c) after a $180^\circ_{x'}$ pulse. The wavy line along the x'-axis indicates the direction of the effective $\boldsymbol{B}_1$ field.

If $\boldsymbol{B}_1$ is along the direction of the y'-axis, as in experiments that we shall meet in Chapters 8 and 9, we speak of a $90^\circ_{y'}$ or a $180^\circ_{y'}$ pulse; in the vector diagrams the wavy line is then along the y'-axis of the rotating coordinate system.

From these vector diagrams it is seen that the transverse magnetization $M_{y'}$ is greatest immediately after a $90^\circ_{x'}$ pulse, and is zero for $\Theta_{x'} = 0°$ or 180°. The transverse component $M_{y'}$ is crucial for the observation of an NMR signal, since the receiver coil is orientated with its axis along the y-direction, and as a consequence of the detection method used a signal proportional to $M_{y'}$ is induced in it. This signal is a maximum for a $90^\circ_{x'}$ pulse, whereas for a $180^\circ_{x'}$ pulse no signal can be observed.

Without going into the details, this can be illustrated by the following experiment. Equation (1-14) shows that the pulse angle can be increased either by increasing the amplitude of the pulse component B_{1i} or by increasing the pulse duration τ_P. To obtain the results reproduced in Figure 1-11 we kept B_{1i} constant and increased the pulse duration τ_P in steps of 1 μs; the sig-

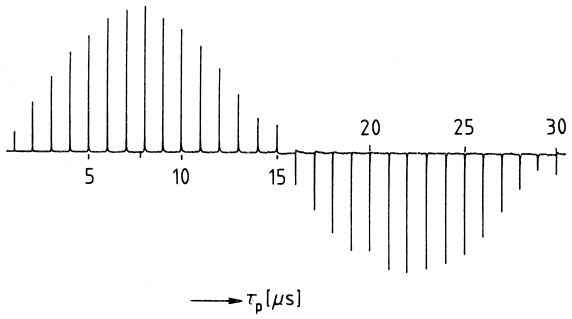

Figure 1-11.
Dependence of the NMR signal from a water sample on the pulse angle Θ. In the experiment the pulse duration τ_P was increased in 1 μs steps. The maximum signal amplitude is obtained with a 90° pulse, which in this case corresponds to a pulse duration of about 8 μs. For τ_P = 15 to 16 μs the signal amplitude is zero, as the pulse angle is then 180°. For still longer pulses the signal amplitude is negative.

nal recorded in each case is shown. The signal amplitude passes through a maximum at a τ_P value of about 7 to 9 μs, then again falls and is approximately zero at $\tau_P \approx$ 15 to 16 μs. The maximum corresponds to a pulse angle of 90°, and where the signal passes through zero the pulse is 180°. The experiment also shows that the time interval τ_P needed for a 90° pulse must be doubled to give a 180° pulse.

For still greater values of τ_P a signal is again observed, but with negative amplitude, i. e. it appears in the spectrum as an inverted peak. From the vector diagram we can understand why this is so: for a pulse angle greater than 180° a transverse component $-M_{y'}$ in the direction of the negative y'-axis appears, inducing a negative signal in the receiver coil.

Up to now we have described, with the help of vector diagrams (Fig. 1-10), the effects of the pulses on the macroscopic magnetization vector $\boldsymbol{M}_0$. But what has become of the $N = N_\alpha + N_\beta$ individual spins which together make up $\boldsymbol{M}_0$? The condition of the spin system after the $180^\circ_{x'}$ pulse is easy to visualize: the populations N_α and N_β have been exactly reversed by the experiment, so that there are now more nuclei in the upper than in the lower energy level. However, to describe the situation after the $90^\circ_{x'}$ pulse is more complicated. In this case $M_z = 0$, and the two Zeeman levels are equally populated. However, this situation differs from that of saturation which was mentioned earlier (see Section 1.4.1), because after the $90^\circ_{x'}$ pulse a magnetization in the y'-direction is present, whereas in saturation it is not. The way in which this transverse magnetization comes about can be understood by the following picture: under the influence of the $\boldsymbol{B}_1$ field the individual nuclear dipoles no longer precess with their axes in a uniform random distribution over the surface of the double cone, but instead a (small) fraction precess in phase, bunched together. This condition is referred to as *phase coherence* (Fig. 1-12; see also Section 7.3).

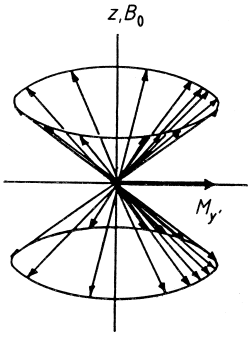

Figure 1-12.
Pictorial representation of phase coherence: after a $90^\circ_{x'}$ pulse a fraction of the nuclear spins (not all!) are bunched together in phase as they precess about the field direction z.

1.5.3 Relaxation

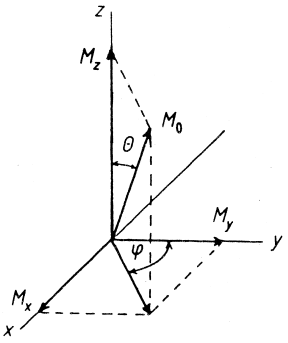

Figure 1-13.
The macroscopic magnetization vector $\boldsymbol{M}_0$, after being turned from its equilibrium orientation through an angle Θ by applying a pulse, now precesses with the Larmor frequency ν_L. At the instant t it has the coordinates M_x, M_y and M_z, in the stationary coordinate system.

At the instant when the pulse is switched off the magnetization vector $\boldsymbol{M}_0$ is deflected from its equilibrium position through an angle Θ. $\boldsymbol{M}_0$, like the individual spins, precesses about the z-axis with the Larmor frequency ν_L; its orientation at any instant is specified in the stationary coordinate system by the three components M_x, M_y and M_z, which vary with the time t (Fig. 1-13).

The spin system now reverts to its equilibrium state by relaxation, with M_z growing back to its original value M_0, while M_x and M_y approach zero. The rather complicated motion of the magnetization vector, both during the application of the radiofrequency field and in the subsequent relaxation, was mathematically analyzed by F. Bloch. He assumed that the relaxation processes were first-order and could be described by two different relaxation times T_1 and T_2. The analysis leads to a set of equations (or a single vector equation) which describe the variation with time of M_x, M_y and M_z. If, instead of the stationary coordinate system x, y, z, we use a rotating coordinate system x', y', z which rotates at the Larmor frequency (see previous section) the equations become much simpler, as they no longer include the precession about the z-axis. For the situation after the pulse has been switched off ($B_1 = 0$), this gives the Bloch equations for relaxation in the rotating frame:

$$\frac{dM_z}{dt} = -\frac{M_z - M_0}{T_1} \tag{1-15}$$

$$\frac{dM_{x'}}{dt} = -\frac{M_{x'}}{T_2} \quad \text{and} \quad \frac{dM_{y'}}{dt} = -\frac{M_{y'}}{T_2} \tag{1-16}$$

T_1 is the *spin-lattice* or *longitudinal relaxation time*, while T_2 is the *spin-spin* or *transverse relaxation time.*

The reciprocals T_1^{-1} and T_2^{-1} of the relaxation times correspond to the rate constants for the two relaxation processes.

To illustrate how simple the description of relaxation becomes in the rotating coordinate system, we will use the above equations to consider what happens to the transverse magnetization after a $90^\circ_{x'}$ pulse.

After the pulse $\boldsymbol{M}_0$ lies along the y'-axis at the instant $t = 0$ (Fig. 1-14a). Consequently $M_0 = M_{y'}$. Since the y'-axis rotates at the Larmor frequency of the nuclei, the transverse magnetization in the y'-direction remains constant, or more exactly, its magnitude only decreases with time at a rate determined by the loss through relaxation. As a result of this relaxation the precessing dipoles, which are at first bunched together (see

Figure 1-12), gradually fan out, so that $M_{y'}$ becomes smaller and eventually zero. This is shown schematically by the vector diagrams in Figure 1-14 b and c. Here the magnetic moments of the individual spins are represented by showing only their components in the x', y' plane (thin arrows). According to Equation (1-16) this decrease is exponential (Figure 1-14 d), and its rate is determined by the transverse relaxation time T_2.

In the discussion of one- and two-dimensional pulse techniques in Chapters 8 and 9 we shall return in detail to the question of the motion of the vectors in the stationary and rotating coordinate systems. The phenomenon of relaxation will be treated in Chapter 7.

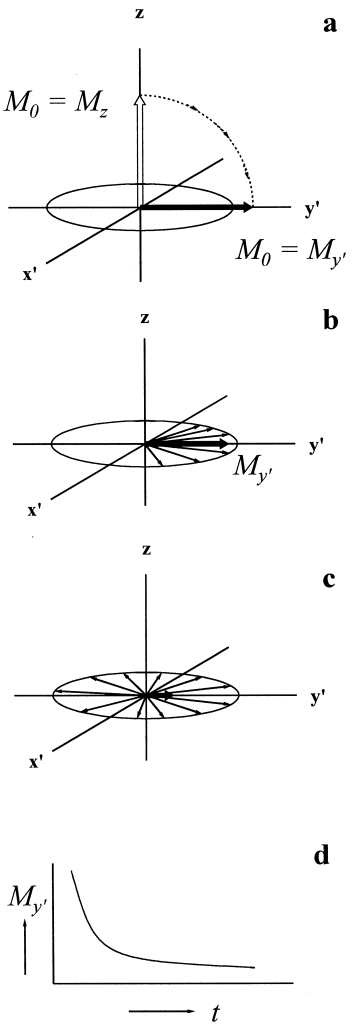

Figure 1-14.
Transverse or spin-spin relaxation. A $90^\circ_{x'}$ pulse turns $\boldsymbol{M}_0$ into the y'-direction (a), then the bunched precessing nuclear dipoles gradually fan out due to spin-spin relaxation (b and c). Diagram d shows the exponential decay of the transverse magnetization component $M_{y'}$.

1.5.4 The Time and Frequency Domains; the Fourier Transformation

The signal detected by the NMR spectrometer following a pulse is determined by $M_{y'}$, but it does not normally look like the decay curve shown in Figure 14 d. Because of the detection method used, such a curve would only be obtained if the generator frequency ν_1 and the resonance frequency of the observed nuclei accidentally coincided. Instead the receiver produces a curve like that shown for CH_3I (**1**) in Figure 1-15. The envelope of this curve corresponds to the curve of Figure 1-14 d. In this example, where there is only a single resonance frequency for the three equivalent protons of the methyl group, the time interval between successive maxima is $1/\Delta\nu$, the reciprocal of the difference in frequency between ν_I and the resonance frequency ν_i of the nuclei. This decay of the transverse magnetization as detected in the receiver is called the free induction decay (FID).

If the sample contains nuclei with different resonance frequencies, or if the spectrum consists of a multiplet as a result of spin-spin coupling (see Section 1.6), the decay curves of the different transverse magnetization components are superimposed and interference between the FIDs occurs. Figure 1-16 A shows such an interferogram for the ^{13}C resonance of $^{13}CH_3OH$ (**2**). This interferogram contains the resonance frequencies and intensities which are of interest to us. However, we cannot analyze the interferogram directly, as we are accustomed to interpreting spectra in the frequency domain rather than in the time domain. Nevertheless, the two spectra can each be derived from the other by a mathematical operation called the *Fourier transformation* (FT):

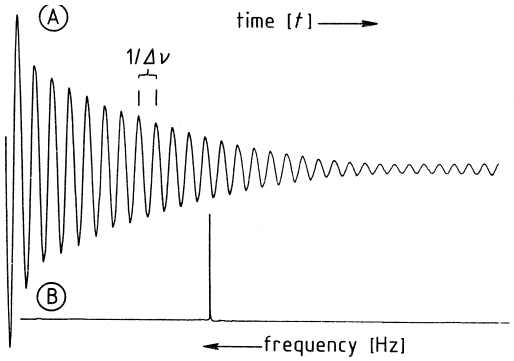

Figure 1-15.
90 MHz ^{1}H NMR spectrum of methyl iodide CH_3I (**1**); one pulse, spectral width 1200 Hz, 8 *K* data points, acquisition time 0.8 s. A: time domain spectrum (FID); the generator frequency is almost exactly equal to the resonance frequency of the sample; B: frequency domain spectrum obtained by Fourier transformation of A.

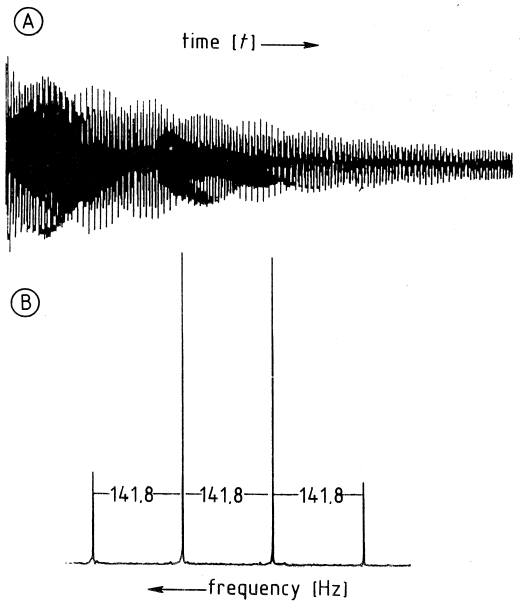

Figure 1-16.
22.63 MHz ^{13}C NMR spectrum of methanol $^{13}CH_3OH$ (**2**); solvent: D_2O, 17 pulses, spectral width 1000 Hz, 8 *K* data points. A: Time domain spectrum (FID); B: frequency domain spectrum obtained by Fourier transformation of A. This consists of a quartet, as the ^{13}C nucleus is coupled to the three protons of the methyl group.

$$g(\omega) = \int_{-\infty}^{+\infty} f(t)e^{-i\omega t}\mathrm{d}t \qquad (1\text{-}17)$$

$f(t)$ corresponds to the spectrum in the time domain, and $g(\omega)$ to that in the frequency domain. $g(\omega)$ is a complex function, i. e. it consists of a real part *Re* and an imaginary part *Im*. In principle it is equally valid to display the spectrum by using either the real part or the imaginary part, since both represent the frequency spectrum. However, the phases of the signals differ by 90°, and thus in the first case an *absorption mode* signal is obtained, whereas in the second case one has a *dispersion mode* signal. In one-dimensional NMR spectroscopy it is usual to represent the spectrum by the real part and thus to display absorption mode signals (Fig. 1-17).

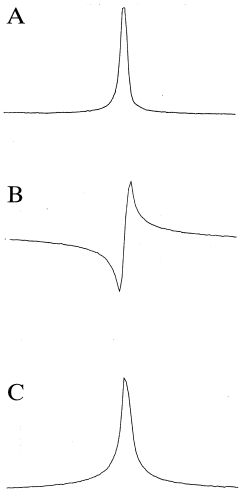

Figure 1-17.
A: Absorption signal
B: Dispersion signal
C: "Absolute value" signal

Because of the method of detection used one usually obtains after the Fourier transformation signals containing both absorption and dispersion components. However, by means of a mathematical operation called phase correction the dispersion component can be removed, so that all the signals in the spectrum are of the usual absorption form.

Figures 1-15 B and 1-16 B show the phase-corrected frequency spectra obtained by Fourier transformation of the interferograms 1-15 A and 1-16 A. The ^{1}H NMR spectrum of methyl iodide consists of a singlet, whereas the ^{13}C spectrum of $^{13}CH_3OH$ is a quartet.

In two-dimensional NMR spectroscopy, for example in displaying COSY spectra, one often uses the "absolute values" of the signals, thus giving the "magnitudes spectrum" M. For this purpose the spectrum is computed by using the expression $M = \sqrt{Re^2 + Im^2}$. This too gives a frequency spectrum with absorption-type signals, but the peaks computed in this way have a broader base than those computed from the real component. However, the great advantage of this form of presentation is that no problems arise from any phase differences between the signals that may occur. We shall return to this problem in Section 9.4.2.

The theory of the Fourier transformation, descriptions of computer programs for performing FT calculations, and other details of the technique can be found in the specialist literature cited in Section 1.8 under "Additional and More Advanced Reading".

1.5.5 Spectrum Accumulation

Usually the intensity of an individual FID is so weak that after Fourier transformation the signals are very small compared with the noise. This is especially so for nuclides with low sensitivity and low natural abundance (e. g. ^{13}C or ^{15}N), or for very dilute samples. Therefore the FIDs of many pulses are added together (accumulated) in the computer, and only then transformed. In this accumulation the random electronic noise becomes partly averaged out, whereas the contribution from the signals is always positive and therefore builds up by addition. The signal-to-noise ratio S : N increases in proportion to the square root of the number of scans NS:

$$S : N \sim \sqrt{NS} \qquad (1\text{-}18)$$

The accumulation of many FIDs – sometimes many hundreds of thousands over a period of several days – calls for very precise field-frequency stability and requires that the data from each

FID are stored in the exactly corresponding memory addresses in the computer. Any variation, including also that of temperature, causes a line broadening and a consequent loss of sensitivity (S : N). The device whose task is to ensure the necessary field-frequency stability is called the lock unit. This uses a separate radiofrequency channel to measure a nuclear resonance other than that of the actual NMR experiment; most commonly it is the ^2H resonance of the deuterated solvent. For this one needs a transmitter which excites the deuterium resonance (using pulses), a receiver and amplifier, and a detector (signal processor). If the magnetic field strength or the frequency changes, the resonance condition is no longer exactly satisfied, causing a reduction of the signal intensity. The lock unit responds to this automatically, by applying a field correction until the resonance condition is restored. Having thus achieved field-frequency stability for the solvent, we can assume that the same stability condition also applies for the nuclei in the dissolved molecules.

The lock signal can also be displayed on the monitor screen when needed, and it is the normal practice to use it for optimizing the magnetic field homogeneity, either manually or automatically. This is achieved by means of a "shim" unit as described in Section 1.5.6, and the procedure of making the necessary adjustments is called "shimming" in everyday laboratory jargon.

Recording an FID and storing it in digital form requires a certain length of time, which is called the *acquisition time*, and is proportional to the number of memory locations used. The number of locations chosen depends on the width of the spectrum, and it is therefore not possible to specify values which are universally valid. For a spectrum with a width of 5000 Hz and 8 K memory locations, for example, about 1 second is needed to store the data (1 K = 2^{10} = 1024). This is also the shortest possible time interval between two successive pulses (the pulse interval). The system is already starting to undergo relaxation during the storage of the data, as can be observed directly on the oscilloscope (Figs. 1-15 A and 1-16 A).

Because the magnetization decreases with time owing to relaxation, the interferogram contains a higher proportion of noise at the end of the acquisition than at the beginning. The rate at which the FID decays is determined by the relaxation time T_2 and by field inhomogeneities (ΔB_0). This fact is particularly important when choosing the pulse interval for the experiment, since in order to make precise intensity measurements the system must be fully relaxed, i. e. must return to the equilibrium condition, before each new pulse. In practice, however, in order to use the time most efficiently, the next pulse usually follows soon after the collection and storage of the FID data, before equilibrium has been established. This means, firstly, that M_z has not yet reached its equilibrium value M_0, and secondly that

there may still be some residual transverse magnetization components $M_{x'}$ and $M_{y'}$ in the x', y' plane. Usually one is prepared to accept this disadvantage, but in some cases, especially in two-dimensional experiments, the residual transverse magnetization can cause artefacts.

An elegant solution which eliminates these unwanted transverse magnetization components is to use pulsed field gradients. Field gradients have long been used in magnetic resonance tomography (see Chapter 14), but their use in high-resolution NMR spectroscopy only became possible when spectrometers began to be equipped with the appropriate hardware, which includes special gradient coils within the probe-head. The method of pulsed field gradients (PFG) has now developed into a very important tool of modern NMR spectroscopy, and therefore it will be described in detail later, in Section 8.3.

1.5.6 The Pulsed NMR Spectrometer

NMR spectrometers are expensive instruments, as the experiment imposes exacting requirements on both the homogeneity and the stability of the magnet and on the performance of the electronics. In the context of this book it would be neither practicable nor appropriate to describe in detail the construction and mechanism of operation of a pulsed NMR spectrometer. The discussion which follows will therefore only briefly outline some of the basic points.

Figure 1-18 shows in schematic form the construction of a pulsed NMR spectrometer. Its components are the cryomagnet, the probe-head, the console, which contains all the associated electronics, and the computer.

The Magnet: A very important component of every NMR spectrometer is the magnet (**1**), shown here in the form of a cutaway vertical section through the cylindrical-shaped assembly. The quality of the magnet plays a key role in determining the quality of the experimental measurement, and therefore of the final spectrum. Until the early 1960s permanent magnets or electromagnets were used, giving flux densities up to 1.41 T (corresponding to an observing frequency of 60 MHz for protons); nowadays, however, by using cryomagnets it is possible to reach flux densities as high as 21.14 T, giving a frequency of 900 MHz for protons. Table 1-2 lists typical magnetic flux densities B_0 and the corresponding ^{1}H and ^{13}C resonance frequencies for NMR spectrometers that have been used in the past and for modern instruments. Very few spectrometers operating below 4.7 T (200 MHz for ^{1}H) remain in use, and all modern instru-

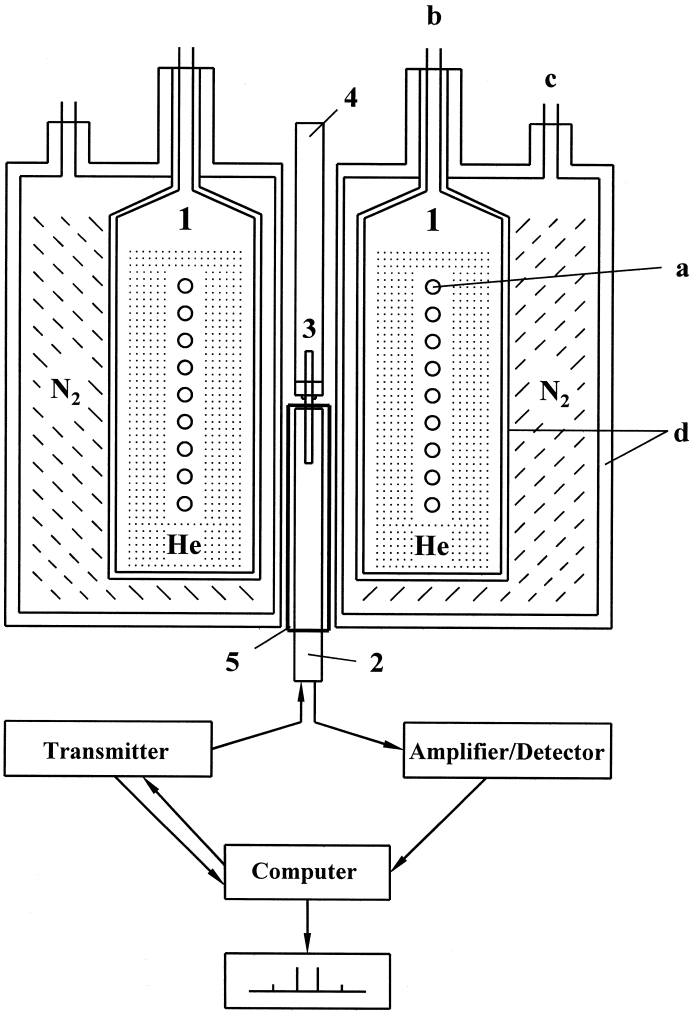

Figure 1-18.
Schematic diagram showing the components of an NMR spectrometer with a cryomagnet. 1 cryomagnet assembly; a magnet coils; b, c filling columns for liquid helium and liquid nitrogen respectively; d vacuum jackets of the inner and outer Dewar vessels; 2 probe-head; 3 sample; 4 sample changer; 5 shim coils.

ments are equipped with cryomagnets. With these magnets the magnetic field $\boldsymbol{B}_0$ is directed along the axis of the sample tube.

The Probe-Head: The heart of an NMR spectrometer is the probe-head (**2**), into which the sample is inserted. It contains the transmitter and receiver coils, together with additional coils for decoupling, for the lock, and for generating field gradients, and also a preamplifier. The probe-head is introduced into the bore of the magnet from below. The diameter of the bore is usually 5 cm.

The sample (**3**) is usually contained in a glass sample tube with an external diameter of 5 mm and a length of about 20 cm, and is introduced into the probe-head from above by means of a sample changer (**4**). When necessary, one can ensure the most efficient utilization of the spectrometer by using an automatic sample changer which can accommodate 50 samples, thus allowing unattended operation overnight or during the

weekend, for example. The turbine for spinning the sample (see below) and the shim coils for optimizing the field homogeneity can also be considered, in a broad sense, as belonging to the probe-head. These are housed in a separate tube which is concentric with the actual probe-head, but remains in the magnet when the probe-head is changed. Usually the sample tube is rotated rapidly about its longitudinal axis, which improves the effective field homogeneity. The sample spinning device (turbine) is at the upper end of the shim tube. In the latest generation of instruments the field homogeneity is so good that sample spinning is not always necessary, and this has made it possible to perform experiments with pulsed field gradients.

The Transmitter: The transmitter consists of a radiofrequency generator and a frequency synthesizer, which provides the various frequencies needed for the NMR experiment (the observing frequency ν_1, and the decoupling and lock frequencies), by deriving all these from a fixed frequency generated by a quartz crystal oscillator. The transmitter also produces pulses of the required duration and power. All these functions are controlled by the computer.

The Receiver: As explained earlier in Section 1.5.2, a radiofrequency voltage proportional to the transverse magnetization $M_{y'}$ is induced in the receiver coil. Its frequency corresponds to the energy of the NMR transition [see Eq. (1-11)], typically several hundred MHz. In general, because the transmitter pulse can excite nuclear spins with slightly different precession frequencies in the sample, the induced voltage does not have a pure single frequency, but a spread of frequencies determined by the chemical shifts (see next section), typically within a narrow range of a few kHz above or below the transmitter reference frequency ν_1. After receiving an initial boost from the preamplifier within the probe-head, the signal must be further amplified and processed. For technical reasons it is preferable and easier to handle frequencies that are considerably lower than ν_1, and therefore the method of detection employs a useful trick which is standard practice in radio reception: using the frequency ν_1 as a reference base, a separate generator (in radio parlance the "local oscillator") provides a new frequency $\nu_1 + \nu_{\text{i.f.}}$, where $\nu_{\text{i.f.}}$, called the intermediate frequency, is typically only a few MHz (i.e., much lower than ν_1). The local oscillator frequency is "mixed" with the radiofrequency NMR signal to form a new signal whose frequency is the difference between the two. Most of the required amplification can then be carried out conveniently and efficiently by an amplifier designed to handle this intermediate frequency (i.f.). A phase-sensitive detector then compares the amplified i.f. signal with an i.f. reference voltage derived from the local oscillator, resulting in a signal made up of relatively low frequencies which are the differences between ν_1 and the frequencies picked up by the

receiver coil. After further amplification by a low-frequency broad-band amplifier, this interferogram or FID (like the examples seen earlier in Figures 1-15 A and 1-16 A) is sent to the computer for processing.

In this method of detection the FID and the frequency-domain spectrum derived from it are determined only by the absolute values of the differences between the signal and reference frequencies, and consequently the system cannot distinguish between a signal at a frequency higher than ν_1 and one at a frequency lower than ν_1 by the same amount. Thus, if two signals fortuitously had frequencies equidistant from ν_1, one higher and one lower, we would obtain only one signal in the spectrum. To avoid this it is necessary to position the reference frequency ν_1 off one end of the spectrum rather than in the middle of it. However, this has two disadvantages: firstly that one half of the frequency band determined by the pulse duration τ_P (see Section 1.5.1) remains unused, and secondly that the electronic noise from this unused part becomes "folded back" into the spectrum. Both these effects result in a considerable sacrifice of sensitivity. To avoid this, most modern pulse spectrometers use *quadrature detection*. This method employs two phase-sensitive detectors, one to measure $M_{y'}$, the y'-component of the magnetization vector, and the second to simultaneously measure $M_{x'}$, the x'-component, which is shifted 90° relative to the first. When both these components are used in the Fourier transformation, their different phases make it possible to differentiate between signals whose frequencies lie above and below the reference frequency. It then becomes possible to position ν_1 in the middle of the spectral region to be observed, thus increasing the sensitivity by a factor $\sqrt{2}$.

The Computer: The interferogram emerging from the final amplifier contains the information of the NMR spectrum in analog form. Before one can obtain the spectrum in the usual frequency-domain form, the information must first be digitized. Measurements of the amplitude of the interferogram (voltage values) are taken at regular time intervals, converted into digital form, and stored in the computer (see Section 1.5.5, Spectrum Accumulation). The Fourier transformation is then carried out in a matter of seconds. In order to ensure that the NMR signals appear at their correct frequencies in the Fourier-transformed spectrum, the sampling interval must be short enough to give at least two data points within each period of the highest frequency component present in the interferogram. If this condition is not satisfied, the computer will treat that component as if it were one of lower frequency, so that the signal becomes back-folded in the spectrum, appearing in a position where there should not actually be a signal. The highest frequency that can be correctly handled by the system is called the *Nyquist frequency.*

Until comparatively recently the main tasks that the computer had to perform were limited to data storage and Fourier transformation. In modern instruments, however, the computer is used to control nearly all the functions of the spectrometer. These include loading programs and setting parameters for the particular experiments that one wishes to perform, automatic shimming, the analysis, simulation, prediction and interpretation of spectra, and very much more. Nowadays it is also possible for the spectrometer's computer to be linked into a network, so that FIDs and other data can be called up remotely from another workstation, where they can be processed independently [4].

1.6 Spectral Parameters: a Brief Survey

1.6.1 The Chemical Shift

1.6.1.1 Nuclear Shielding

The discussion up to this point would lead one to expect only one nuclear resonance signal for each nuclear species. If this were really so the technique would be of little interest to the chemist.

Fortunately, however, the resonances are influenced in characteristic ways by the environments of the observed nuclei. Just to make things simpler we have up to now assumed that we are dealing with isolated nuclei. However, the chemist is concerned with molecules, in which the nuclei are always surrounded by electrons and other atoms. The result of this is that in diamagnetic molecules the effective magnetic field B_{eff} at the nucleus is always less than the applied field B_0, i.e. the nuclei are shielded. The effect, although small, is measurable. This observation is expressed by Equation (1-19):

$$B_{\text{eff}} = B_0 - \sigma B_0 = (1 - \sigma) B_0 \qquad (1\text{-}19)$$

Here σ is the *shielding constant*, a dimensionless quantity which is of the order of 10^{-5} for protons, but reaches larger values for heavy atoms, since the shielding increases with the number of electrons. It should be noted that σ-values are molecular constants which do not depend on the magnetic field. They are determined solely by the electronic and magnetic environment of the nuclei being observed.

The resonance condition, Equation (1-12), thus becomes:

$$\nu_1 = \frac{\gamma}{2\pi} (1 - \sigma) B_0 \qquad (1\text{-}20)$$

The resonance frequency ν_1 is proportional to the magnetic flux density B_0 and – more importantly for our purpose – to the shielding factor $(1 - \sigma)$. From this statement we arrive at the following important conclusion: nuclei that are chemically non-equivalent are shielded to different extents and give separate resonance signals in the spectrum.

The 90 MHz ^{1}H NMR spectrum (B_0 = 2.11 T) of a mixture of bromoform ($CHBr_3$, **3**), methylene bromide (CH_2Br_2, **4**), methyl bromide (CH_3Br, **5**) and tetramethylsilane (TMS, $Si(CH_3)_4$, **6**), recorded by the frequency sweep method (see Section 1.4.2), is reproduced in Figure 1-19. The signal of TMS appears at exactly 90 000 000 Hz = 90 MHz; the signals of the other compounds are found at 90 000 237 Hz (CH_3Br), 90 000 441 Hz (CH_2Br_2) and 90 000 614 Hz ($CHBr_3$). Thus the proton in bromoform has the highest measured resonance frequency and the protons in TMS the lowest. It follows from the resonance condition, Equation (1-20), that the protons are least shielded in bromoform and most shielded in TMS, i. e.:

$$\sigma\,(CHBr_3) < \sigma\,(CH_2Br_2) < \sigma\,(CH_3Br) < \sigma\,(TMS)$$

In accordance with a universal convention, resonance signals in NMR spectroscopy are recorded in such a way that the shielding constant σ increases from left to right.

(In a spectrum recorded by the field sweep method – constant frequency ν_1 and variable flux density B_0 – to keep the signals in the same sequence on the abscissa the magnetic flux density must increase from left to right. Because of this fact it is customary for historical reasons to use expressions such as "a signal appears at higher field", or "a signal is at lower field").

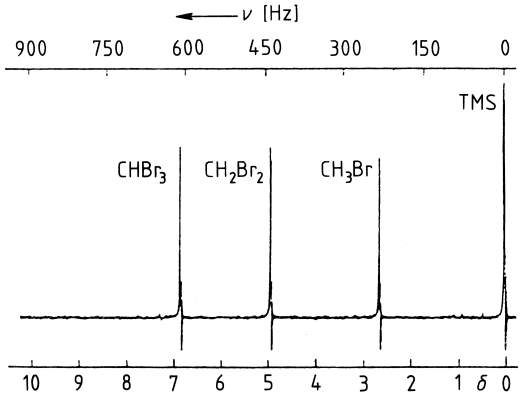

Figure 1-19.
90 MHz ^{1}H NMR spectrum of a mixture of $CHBr_3$ (**3**), CH_2Br_2, (**4**), CH_3Br (**5**) and TMS (**6**).

1.6.1.2 Reference Compounds and the δ-Scale

In Figure 1-19 no absolute values are given for the magnetic flux density B_0 or for the resonance frequencies ν_1, since the measured frequencies are only valid for the experiment carried out with $B_0 = 2.11$ T. In NMR spectroscopy there is, unfortunately, no absolute spectral scale, since the resonance frequency and the magnetic flux density are interdependent as a consequence of the resonance condition (Equation 1-20). A relative scale is therefore used, whereby one measures the frequency difference $\Delta\nu$ between the resonance signals of the sample and that of a reference compound. Modern spectrometers are calibrated in such a way that the separation between the signals can be read off directly in Hz, or printed out directly by the computer.

Before each measurement the reference compound is added to the sample to be examined, and in such cases it is therefore called an *internal standard*. In practice one uses a solvent into which one has previously added a suitable amount of a reference compound. In ^{1}H and ^{13}C NMR spectroscopy tetramethylsilane (TMS) is usually employed for this purpose. TMS is particularly suitable from both the spectroscopic and the chemical points of view. The fact that it contains twelve equivalent, highly shielded protons means firstly that only a small amount needs to be added, and secondly that it gives only a single sharp peak, which is at the right-hand end of the spectrum clearly separated from most other resonances (Fig. 1-19). Moreover, TMS is chemically inert, magnetically isotropic, and non-associating. In addition, because of its low boiling point (26.5 °C), it can be easily removed in cases where the sample needs to be recovered.

If we measure the peak positions in the spectrum shown in Figure 1-19, we obtain for the frequency differences $\Delta\nu$ from TMS as internal standard the values 614, 441 and 237 Hz respectively for bromoform, methylene bromide and methyl bromide. With modern spectrometers all the line positions are calculated by Fourier transformation and the frequencies are printed out directly.

But the $\Delta\nu$-values also depend on B_0! One therefore defines a quantity δ, the *chemical shift*, as follows:

$$\delta_{\text{sample}} = \frac{\nu_{\text{sample}} - \nu_{\text{reference}}}{\nu_{\text{reference}}} \qquad (1\text{-}21)$$

As the numerator in this expression is typically no more than a few hundred Hz, whereas the denominator is usually several hundred MHz, the δ-value defined in this way is in general a very small number, and therefore δ-values are instead given in

parts per million (ppm). Thus, Equation (1-21) is replaced by Equation (1-22), where $\Delta\nu$ is given in Hz and $\nu_{reference}$ in MHz:

$$\delta_{sample}\ [ppm] = \frac{\Delta\nu}{\nu_{reference}} \frac{[Hz]}{[MHz]} \qquad (1\text{-}22)$$

The convention of introducing a factor of 10^6 to give more convenient numbers and quoting δ-values in parts per million was included in a recommendation issued by IUPAC in 1972. But as ppm is not a unit of measurement in the sense of a dimension, IUPAC also recommended then that δ-values in this form should not be followed by "ppm" (since the factor of 10^6 was already contained in the definition of δ). However, that recommendation did not find general acceptance among NMR spectroscopists. Therefore, in 2001 the IUPAC Committee issued a new recommendation, namely that the chemical shift should be defined as in Equation (1-22), and that quoted δ-values should also be described as "ppm". Accordingly, that procedure is followed throughout this book.

The δ-value for the reference compound TMS is, by definition, zero, since in this case $\Delta\nu = 0$; thus:

$$\delta\ (TMS) = 0\ ppm \qquad (1\text{-}23)$$

The δ-values, starting from the TMS signal, are positive to the left and negative to the right of it.

Examples:

○ For the three compounds of Figure 1-19 we calculate the following chemical shifts:

$$\delta\ (CHBr_3) = \frac{614}{90 \times 10^6} = 6.82\ ppm$$

$$\delta\ (CH_2Br_2) = \frac{441}{90 \times 10^6} = 4.90\ ppm$$

$$\delta\ (CH_3Br) = \frac{237}{90 \times 10^6} = 2.63\ ppm$$

From the δ-values we can, by using Equation (1-22), calculate the interval in Hz between the resonance and the TMS signal for any arbitrary observing frequency. Thus, assuming in our example an observing frequency of 300 MHz these intervals are:

$CHBr_3$: $\Delta\nu = 2046$ Hz
CH_2Br_2: $\Delta\nu = 1470$ Hz
CH_3Br : $\Delta\nu = 789$ Hz

It is not always possible to add TMS to the sample under examination. For example, TMS is insoluble in water. In such cases a different reference compound is added to the sample and the results are converted to the TMS scale. Occasionally too an *external standard* is used. This is a reference compound which is sealed into a capillary and its resonance recorded

along with that of the sample. For this purpose it is best to use special coaxial sample tubes which are commercially available. However, in calculations using such data and for comparing with literature values one must take into account the fact that the nuclei at the position of the reference standard experience a different shielding from those in the sample. For reference compounds of "other" nuclides see [1].

The relationships between chemical shifts and molecular structure will be described in detail in Chapter 2, and the chemical shifts of "other" nuclides apart from ^{1}H and ^{13}C will also be discussed.

1.6.2 Spin-Spin Coupling

1.6.2.1 The Indirect Spin-Spin Coupling

In the mixture of $CHBr_3$, CH_2Br_2, CH_3Br and TMS (**3–6**) we observe a singlet for each compound (Fig. 1-19), since each compound contains only one group of chemically equivalent protons. This is an unusual example; in general most of the signals exhibit a fine structure. Figure 1-20 shows a simple example, the spectrum of ethyl acetate (**7**). From left to right we see a quartet, a singlet, a triplet, and the TMS signal. The protons within each group are certainly chemically equivalent, and therefore the splitting of the signals cannot be caused by any differences of chemical type between individual protons. The cause of this fine structure will be explained below by taking examples from ^{1}H NMR spectroscopy, but the same considerations can be extended to ^{13}C and other nuclides with $I = 1/2$.

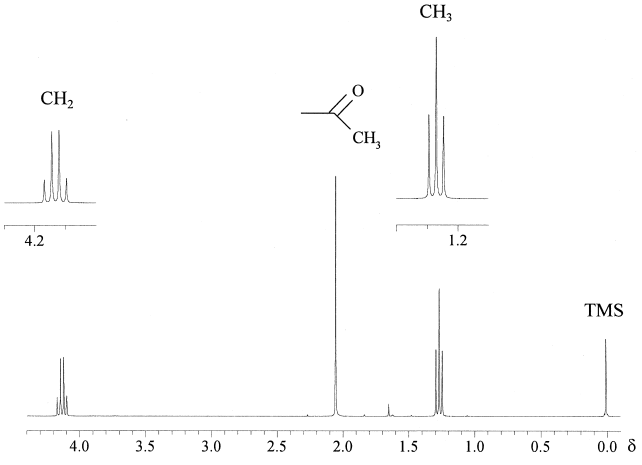

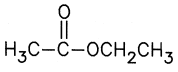

7

Figure 1-20.
300 MHz ^{1}H NMR spectrum of ethyl acetate (**7**) in $CDCl_3$.

Up to now we have taken no account of the fact that neighboring magnetic dipoles in a molecule interact with each other. In the ethyl group of ethyl acetate the two methylene protons are coupled to the three protons of the methyl group. This *spin-spin coupling* affects the magnetic field at the positions of the nuclei being observed. The effective field is stronger or weaker than it would be in the absence of the coupling, and in accordance with Equation (1-20) for the resonance condition this alters the resonance frequencies.

The fine structure seen in Figure 1-20 is caused by the socalled *indirect spin-spin coupling*, indirect because it occurs through the chemical bonds (see Section 3.6).

Nuclear dipoles can also be coupled to each other directly through space. For example, this *direct spin-spin coupling* has an important role in solid-state NMR spectroscopy. In high-resolution NMR spectroscopy, when making measurements on low-viscosity liquids, this coupling is averaged to zero by molecular motions. In the following discussion we will be concerned only with the indirect spin-spin coupling.

Before considering in detail the multiplet structure of the resonances of ethyl group protons, we must first try to understand how the spectrum is altered by the effects of indirect spin-spin coupling, taking the example of two coupled nuclei A and X. Examples of two-spin systems of this type are the molecules **H-F**, ^{13}**CH**Cl$_3$, and Ph–C**H**^{A}=C**H**^{X}COOH. This model will then be extended to multi-spin systems.

1.6.2.2 Coupling to One Neighboring Nucleus (AX Spin System)

In a two-spin system AX, if we consider only the chemical shifts the spectrum consists of two resonance signals with frequencies ν_A and ν_x. If now A and X are coupled to each other, we find two signals for the A-nuclei and two for the X-nuclei (Fig. 1-21).

Let us first confine our attention to the two resonances for A. To understand the splitting into a doublet we must distinguish between two situations. In the first the nucleus X, coupled to A, is in the α-state, and its magnetic moment thus has a compo-

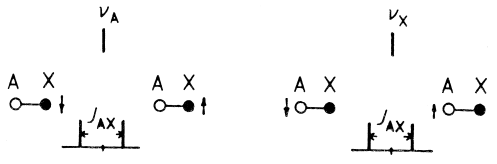

Figure 1-21.
Sketch to explain the fine structure in the spectrum of an AX spin system with a coupling constant J_{AX}. ν_A and ν_X are the resonance frequencies in the absence of coupling.

nent μ_z along the field direction; we represent this by an arrow directed upwards (A-X ↑). If on the other hand X is in the β-state, μ_z points in the negative field direction (A-X ↓; see Section 1.3). The interaction between A and X produces an additional field contribution at the position of A, and for the two states of the X-nucleus the contributions, although equal in magnitude, have opposite signs. In the first situation, therefore, ν_A is shifted to higher frequency by a fixed amount, whereas in the second situation it is shifted to lower frequency by the same amount. We are unable to predict whether an X-nucleus in the α-state will shift the A-resonance to higher or lower frequency. The assignment indicated in Figure 1-21 is arbitrarily chosen. We shall return to this problem in Section 4.3 in connection with the signs of coupling constants.

Since in a macroscopic sample the numbers of molecules with the X-nucleus in the α-state (A-X ↑) and in the β-state (A-X ↓) are nearly equal, two signals of equal intensity appear in the spectrum, i. e. the single peak in the spectrum without coupling is split into a doublet.

An analogous situation applies for the X-nucleus, since the coupling to A similarly causes two X resonances, i. e. a doublet.

The interval between the two lines of each doublet is the same for the A and X parts of the spectrum; it is called the *indirect* or *scalar coupling constant* and is denoted by J_{AX}. Since the splitting is due solely to the nuclear magnetic moments, the value of the coupling constant J_{AX} – unlike the chemical shift – does not depend on the magnetic flux density B_0. It is therefore always given in Hz.

It should be noted that the chemical shift always corresponds to the middle of a doublet, which would be the position of the signal if there were no coupling.

The spectrum of the two olefinic protons of cinnamic acid (**8**, Fig. 1-22) is of the AX type. However, the intensities within the doublet deviate to some extent from the ideal 1 : 1 ratio ("roof effect"). There are two reasons for this: firstly the signals of the proton in the α-position are slightly broadened by coupling to the ring protons, and secondly the spectrum of our two-spin system is in this case not quite of the first-order type. These complications will be discussed in more detail in Sections 1.6.2.8 and 4.3.2.

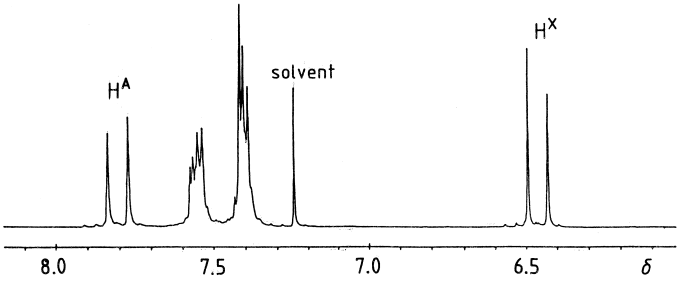

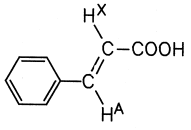

8

Figure 1-22.
Part of the 250 MHz ^{1}H NMR spectrum of cinnamic acid (**8**) in $CDCl_3$; δ (OH) ≈ 11.8 ppm.

1.6.2.3 Coupling to Two Equivalent Neighboring Nuclei (AX_2 Spin System)

As an example of coupling between three nuclei we will consider the three-spin system $C\mathbf{H}^A\text{-}C\mathbf{H}_2^X$. Nucleus A now has two equivalent neighbor nuclei X, for which there are three possible spin orientations in the magnetic field. Considering only the z-components μ_z of the magnetic moments, the two spins of the X-nuclei can be parallel to each other, either along the field direction ($\uparrow\uparrow : \alpha\alpha$) or opposite to the field direction ($\downarrow\downarrow : \beta\beta$), or they can be antiparallel to each other ($\uparrow\downarrow : \alpha\beta$ or $\downarrow\uparrow : \beta\alpha$) (Fig. 1-23). If the X-spins are antiparallel the additional field contributions at the position of nucleus A cancel to zero, and the resonance signal is in the position which it would occupy if there were no coupling. The two parallel spin arrangements cause additional field contributions at the position of A which are equal in magnitude but opposite in sign. This results in two further resonance signals, and a triplet is therefore observed for the protons $\mathbf{H}^A$. The interval between any two adjacent lines is J_{AX}. The intensities are in the ratio 1 : 2 : 1. The middle signal is thus of double intensity, since in a macroscopic sample molecules with an antiparallel arrangement of the X-spins are twice as numerous as those with a parallel arrangement in either one or the other direction.

For the two protons $\mathbf{H}^X$ of the $C\mathbf{H}_2^X$ group we obtain a doublet, as they are coupled to only one neighbor nucleus $\mathbf{H}^A$. The total intensities of the triplet and of the doublet are in the ratio 1 : 2.

The chemical shifts δ_A and δ_X are calculated from the signal positions ν_A and ν_X in the absence of coupling, as was done in the case of the two-spin system AX; ν_A corresponds to the middle signal of the triplet and ν_x to the mid-point of the doublet. As an example Figure 1-24 shows the spectrum of benzyl alcohol (**9**), in which the triplet at $\delta \approx 1.8$ ppm is assigned to the proton

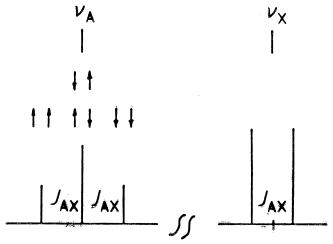

Figure 1-23.
Sketch to explain the splitting pattern observed for a three-spin AX_2 system; the arrows indicate the orientations of the two X spins.

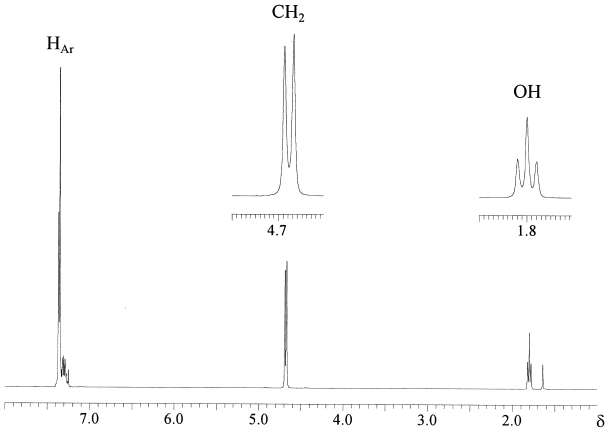

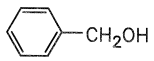

9

Figure 1-24.
300 MHz ^{1}H NMR spectrum of benzyl alcohol (**9**) in $CDCl_3$.

attached to oxygen ($\mathbf{H}^{A}$), and the doublet at $\delta \approx 4.7$ ppm to the two protons of the methylene group ($C\mathbf{H}_2^{X}$).

1.6.2.4 Coupling to Three or More Equivalent Neighboring Nuclei (AX_n Spin System)

The splitting patterns for couplings to three or more equivalent neighboring nuclei can be constructed in the same way as was shown in the previous section for two equivalent neighboring nuclei. If a proton is coupled to three neighbors X, e. g. to the three protons of a methyl group, as in $C\mathbf{H}^{A}\text{-}C\mathbf{H}_3^{X}$, one expects to find for $\mathbf{H}^{A}$ a quartet with the intensity distribution 1 : 3 : 3 : 1 (Fig. 1-25). For the methyl protons $\mathbf{H}^{X}$ one again finds a doublet, since these are coupled to only a single neighbor, $\mathbf{H}^{A}$. A spectrum of this type is obtained for paraldehyde (**10**), which is the trimer of acetaldehyde (Fig. 1-26).

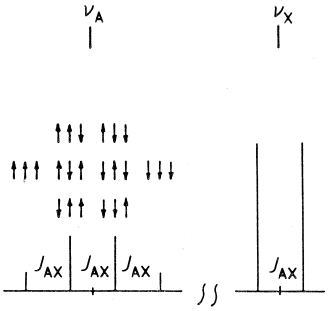

Figure 1-25.
Sketch to explain the splitting pattern observed for a four-spin AX_3 system; the arrows indicate the orientations of the three X spins.

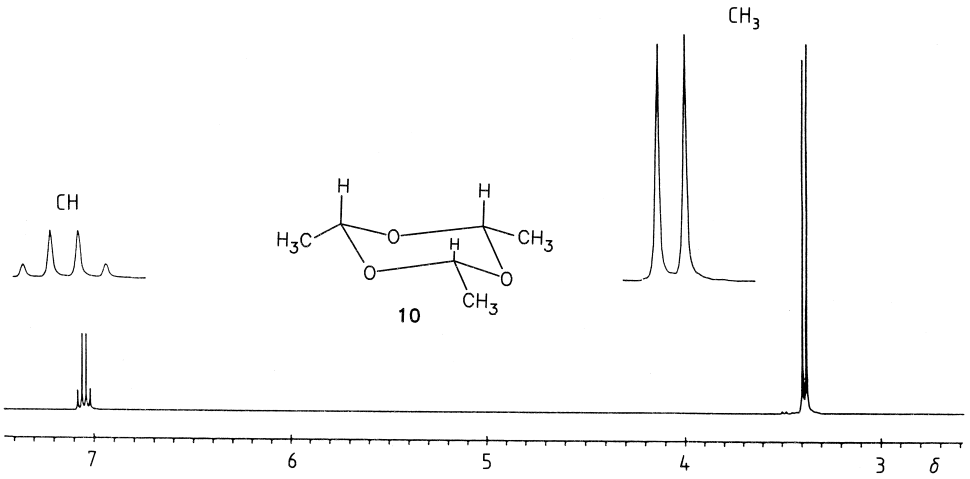

Figure 1-26.
250 MHz ^{1}H NMR spectrum of paraldehyde (**10**). The quartet and doublet are shown expanded, both by the same factor.

1.6.2.5 Multiplicity Rules

The number of lines in a multiplet, which is called the multiplicity M, can be calculated from Equation (1-24):

$$M = 2nI + 1 \qquad (1\text{-}24)$$

Here n is the number of equivalent neighbor nuclei. For nuclei with $I = 1/2$, which includes those that most concern us, Equation (1-24) simplifies to:

$$M = n + 1 \tag{1-25}$$

For couplings to nuclei with $I = 1/2$ the signal intensities within each multiplet correspond to the coefficients of the binomial series, which can be obtained from Pascal's Triangle:

$n = 0$			1			
$n = 1$		1		1		
$n = 2$	1		2		1	
$n = 3$		1		3		3		1
$n = 4$	1		4		6		4		1
⋮			⋮			

We can now understand the splitting patterns for ethyl acetate (**7**) in Figure 1-20. The two methylene protons are coupled to the three equivalent CH_3 protons of the ethyl group, and in accordance with Equation (1-25) they give a quartet ($\delta \approx 4.1$ ppm). The three methyl protons are coupled to the two equivalent protons of the methylene group, which gives a triplet ($\delta =$ 1.3 ppm). Such a combination of a quartet and a triplet in the intensity ratio 2 : 3 always enables one to recognize immediately that the compound being examined contains an ethyl group. Finally, the singlet at $\delta = 2$ ppm in the spectrum of **7** originates from the three methyl protons of the acetyl group.

1.6.2.6 Couplings between Three Non-equivalent Nuclei (AMX Spin System)

Figure 1-27 shows the spectrum of styrene (**11**). Here we are only interested in the signals of the three mutually coupled non-equivalent vinyl protons $\mathbf{H}^A$, $\mathbf{H}^M$ and $\mathbf{H}^X$ (three-spin AMX system).

In the spectrum we find for each proton four signals of nearly equal intensities. The splitting schemes shown above the expanded regions of the spectrum in Figure 1-27 show how the multiplets for each of the protons can be reconstructed and analyzed. One begins by considering the spectrum without coupling, which would consist of three resonance lines at ν_A, ν_M and ν_X. Then one restores one of the couplings for each nucleus – preferably the largest in each case – and splits each line into a doublet corresponding to the coupling constant. This is repeated for the second, smaller, coupling constant, so that each line of the first doublet is further split into a doublet. This leads to a

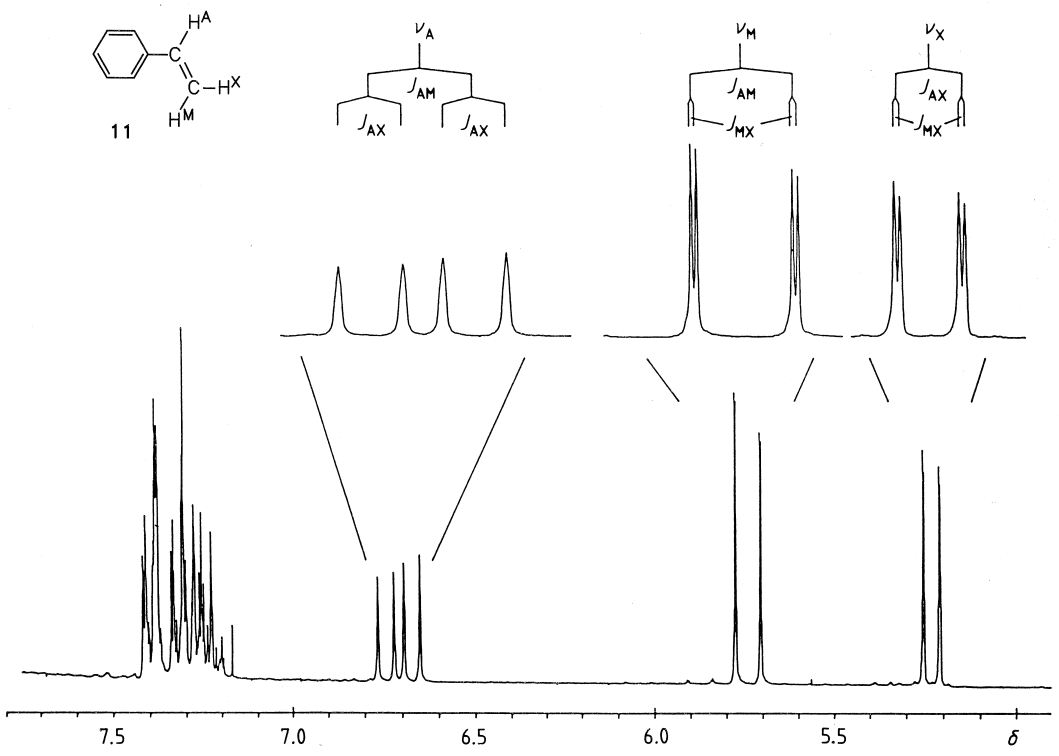

Figure 1-27.
250 MHz ^{1}H NMR spectrum of styrene (**11**) in $CDCl_3$. The protons H^A, H^M and H^X each give a doublet of doublets, shown expanded by the same factor in each case.
J_{AM} = 17.6 Hz, J_{AX} = 10.9 Hz, J_{MX} = 1.0 Hz.

doublet of doublets for each of the protons $\mathbf{H}^A$, $\mathbf{H}^M$ and $\mathbf{H}^X$, whose centers (ν_A, ν_M and ν_X) correspond to the δ-values.

1.6.2.7 Couplings between Equivalent Nuclei (A_n Spin Systems)

Why is it that in the ^{1}H NMR spectrum of an isolated methyl group we find only one signal, even though each proton has as its neighbors two other protons of the methyl group, thereby providing the conditions for coupling to occur? Why does one only find one signal for the six protons of benzene, despite the fact that in benzene derivatives the protons are seen to be coupled to each other?

Exact answers to these questions are provided by quantum-mechanical calculations. Without going into the details of the theory, we shall here merely express this result in the form of a general rule:

Couplings between equivalent nuclei cannot be observed in the spectrum!

In the next section it will become necessary to qualify this rule to some extent, as it applies only to first-order spectra.

In the methyl and methylene groups considered up to now, and in benzene, the protons are equivalent. Consequently the couplings within them cannot be observed, and the spectra are simple and easy to interpret.

1.6.2.8 The Order of a Spectrum

A spectrum which contains only singlets is said to be a *zero-order* spectrum. Most ^{13}C NMR spectra belong to this class as a result of the method of recording which is used (^{1}H broad-band decoupling; see Section 5.3).

If the multiplets can be analyzed according to the rules already given, one is dealing with a *first order* spectrum. Such spectra are to be expected in all cases where the frequency interval $\Delta\nu$ between the coupled nuclei is large compared with the coupling constants, i. e. $\Delta\nu \gg J$. If this condition is not satisfied the intensity ratios within the multiplets alter, and additional lines may appear. Such a spectrum is described as being of *higher order*. These effects will be considered in more detail in Chapter 4. In higher-order spectra the couplings between equivalent nuclei also become evident. The analysis of such spectra is more complicated, and often it is only possible by using a computer. In the course of such an analysis it also emerges that the coupling constants can have either positive or negative sign. However, we shall see (in Section 4.3.1) that the appearance of spectra of the first-order type is not affected by the signs.

1.6.2.9 Couplings between Protons and other Nuclei; ^{13}C Satellite Spectra

In the ^{1}H NMR spectra of organic molecules one normally only sees H,H couplings. However, for molecules containing fluorine, phosphorus or other nuclei which have a magnetic moment, the couplings to these nuclei are also seen. The same rules apply as for H,H couplings. For these heteronuclear couplings there is the additional simplification that $\Delta\nu \gg |J|$, and thus the condition for first-order spectra is nearly always fulfilled.

At this point special mention must be made of the couplings between protons and ^{13}C nuclei. These C,H couplings make themselves apparent in the ^{1}H NMR spectrum by the ^{13}C satellite signals. What are ^{13}C satellites? Figure 1-28 shows the ^{1}H NMR spectrum of chloroform. It consists of a main peak at $\delta = 7.24$ ppm, with two small peaks to the right and left of it (in the figure these are shown greatly amplified). The smaller peaks are caused by the 1.1 % of chloroform molecules that contain a ^{13}C nucleus, i. e. by $^{13}CHCl_3$. The proton is coupled to the ^{13}C nucleus, and this gives a doublet in the ^{1}H NMR spectrum, the ^{13}C *satellites*. The interval between the two satellite peaks is equal to J(C,H) = 209 Hz. The intensity of each satellite is 0.55 % of that of the main peak. (A corresponding doublet with the separation J(C,H) is also observed in the ^{13}C NMR spectrum of chloroform.) The ^{13}C satellite signals are not always so easy to interpret as in the chloroform spectrum (see Section 4.7).

More information on the couplings of protons to "other" nuclei, on heteronuclear couplings that do not involve protons, and on couplings involving nuclei with a spin I greater than 1/2, can be found in Section 3.7.

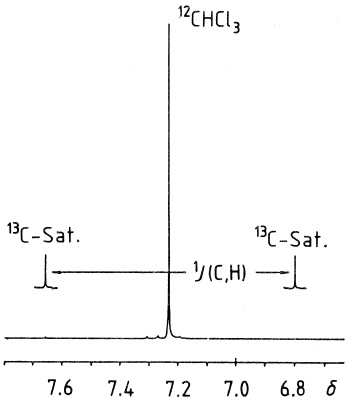

Figure 1-28.
250 MHz ^{1}H NMR spectrum of chloroform; the ^{13}C satellites are shown with a 15-times amplification; ^{1}J(C,H) = 209 Hz.

1.6.3 The Intensities of the Resonance Signals

1.6.3.1 ^{1}H Signal Intensities

The area under the signal curve is referred to as the *intensity* or the *integral* of the signal. Comparing these intensities in a spectrum directly gives the ratios of the protons in the molecule. In the case of multiplets one must, of course, integrate over the whole group of peaks. An example of an integration is shown in Figure 1-29.

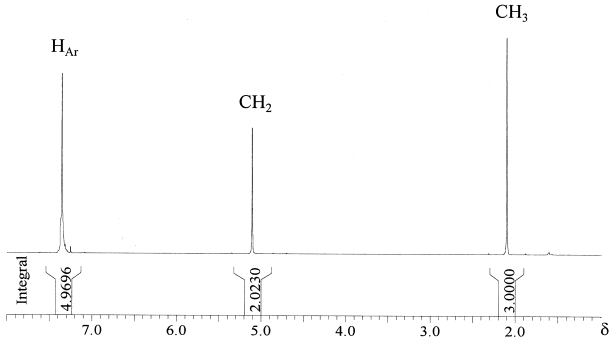

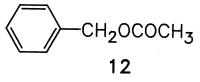

12

Figure 1-29.
300 MHz ^{1}H NMR spectrum of benzyl acetate (**12**) with integrated intensities shown below.

In the ^{1}H NMR spectrum of benzyl acetate (**12**) we find three singlets corresponding to C_6H_5, CH_2 and CH_3. Integration gives the result 5 : 2 : 3 for the ratio of their areas, and from this all the signals can be assigned.

Signal intensities are next in importance to chemical shifts and indirect spin-spin coupling constants as aids to structure determination; they also make possible the *quantitative analysis* of mixtures.

1.6.3.2 ^{13}C Signal Intensities

In principle it should also be possible from the signal intensities in ^{13}C NMR spectra to reach conclusions about the numbers of carbon atoms present in the molecule. However, because of the low natural abundance and sensitivity compared with protons, detection methods are used which have the undesirable side-effect of distorting the integrals. For this reason it is not usual to give integral curves in ^{13}C NMR spectroscopy. The detailed causes of this are as follows:

- The amplitudes of the different frequency components of the pulse become smaller with increasing distance from the transmitter frequency ν_1. Consequently nuclei with different resonance frequencies are excited to varying extents (Section 1.5.1 and Fig. 1-8).
- A resonance peak is not stored in the computer as a complete continuous curve but as a relatively small number of points (Fig. 1-30). In the integration one determines the area bounded by the straight lines joining these points. The closer the spacing of the points the more exact is the integral. The number of data points used in recording the spectrum is usually determined by the time available for the recording. Of the two curves shown in Figure 1-30 one – the broken curve – was recorded with 32 K data points, and the other – the solid curve – was recorded with 2 K data points. Whereas in the broken curve the points are at intervals of about 0.01 Hz, the intervals in the solid curve are more than 0.2 Hz. One can clearly see that the latter curve does not correctly reproduce the line shape. The amplitude is too small, the half-height width is too great, and consequently the integral must also be incorrect. Furthermore, the positions of the maxima in the two curves, from which the δ-values are calculated, differ by about 0.1 Hz. In practice, however, this error is negligible.
- The time interval between two successive pulses during the accumulation is usually so short that the spin system cannot return to equilibrium by relaxation. This leads to incorrect

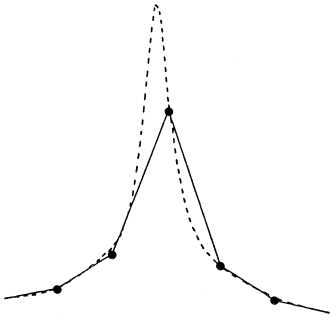

Figure 1-30.
Comparison of the same ^{1}H NMR signal recorded with 32 *K* data points (dashed curve) and with 2 *K* data points (solid line). The dashed curve gives the true line shape. The solid line gives only a distorted peak, with errors in height, width, area and position of maximum.

integrals, the effects being much greater for nuclei with long relaxation times T_1 than for those with a short T_1.

- ^{13}C NMR spectra are normally recorded with ^{1}H broad-band decoupling (Section 5.3). Under these conditions the signals are amplified by the nuclear Overhauser effect (NOE, Chapter 10). The increase in intensity depends on the number of directly bonded hydrogen atoms, and on other factors influencing the relaxation times (Chapter 7).

Every ^{13}C NMR spectrum is affected by all these four sources of error. It is not possible to generalize about the magnitudes of the different effects and of the total integration error – every measurement therefore involves an individual compromise between accuracy and time spent in recording. The causes of incorrect intensity measurement can be completely, or at least partially, avoided by taking precautions with the spectrometer and the recording technique – although at the cost of increased recording times. For *accurate determination of ^{13}C intensities* the following measures are essential:

- The pulse must be of sufficiently high power to ensure that the fall-off of intensity in the frequency components over the full width of the spectrum is negligible. This condition is usually satisfied for ^{1}H spectra, but not for ^{13}C spectra. It is even more critical for other nuclides – ^{31}P for example – for which the spectral width is greater than for ^{13}C.
- Where the spectral width is large and the lines are narrow a computer with a large memory capacity is needed. If a spectrum with a width of 5000 Hz is recorded using 4 K (= 4096) data points the resulting digital resolution is only 1.25 Hz per data point. However, the line widths are usually less than this, so one needs to use 8 K, 16 K or 32 K data points, or alternatively to record spectra of a smaller width, i.e. selected regions of the spectrum.

Errors caused by different relaxation times T_1 and different NOES are more difficult to eliminate; furthermore, these are the largest sources of error. The following methods are available:

- Errors caused by too high a pulse repetition rate can be avoided by inserting a delay equal to 5 T_1 between successive pulses. A spin system needs this amount of time to undergo nearly complete relaxation after a 90° pulse. For relaxation times as long as 100 s, such as are found for quaternary carbon nuclei, this would require a waiting time of 8 to 10 minutes between pulses! In practice such an experiment would be unrealistic, and in these circumstances it is usual to do without intensity measurements.
- If all the sources of error discussed up to now have been eliminated by a suitable choice of experimental conditions,

it becomes worthwhile to suppress the NOE for each quantitative measurement. This can be achieved in two ways:

– Adding paramagnetic ions to the sample solution shortens the relaxation times T_1 (and T_2). Chelate complexes of chromium, such as $Cr(acac)_3$, are generally used for this purpose, but too high a concentration must be avoided as it would broaden the lines (Section 7.3.3). This method is not usually employed, and is especially unsuitable if the sample is needed for further experiments. Another method has therefore been developed, viz.
– A pulse experiment which is the inverse of the gated decoupling described in Section 5.3.2. In this the broadband (BB) decoupler is switched on only during the observing pulse and the subsequent data accumulation. One obtains a decoupled ^{13}C NMR spectrum with the correct intensities, since the NOE is unable to build up during this short time. When the FID has been stored and the BB decoupler switched off, the system must relax again before the next pulse. However, the time needed for this is shorter than 5 T_1.

To summarize, quantitative ^{13}C NMR measurements are possible if the following conditions are ensured:

- high pulse power and small spectral width
- high digital resolution
- a pulse repetition rate that is not too high
- suppression of the NOE.

All the methods described can be carried out without difficulty, but they are very costly in measurement time, and are therefore only used in special circumstances.

1.6.4 Summary

Three types of spectral parameters are obtainable from NMR spectra: chemical shifts, indirect spin-spin couplings, and intensities.

- In this chapter we learned that the chemical shift is caused by the magnetic shielding of the nuclei by their surroundings, mainly by the electrons. The resonance frequencies depend on the magnetic flux density, and for this reason absolute line positions are never specified. Instead we define a dimensionless quantity, the δ-value, which gives the position of the signal relative to that of a reference compound, and also relates it to the measurement frequency. Consequently δ-values are always given in ppm independent of the spectro-

meter used and can be directly compared. The reference compound generally used in ^{1}H and ^{13}C NMR spectroscopy is tetramethylsilane (TMS).

- The interaction between neighboring nuclear dipoles leads to a fine structure. The strength of this interaction is given by the spin-spin coupling constant *J*. Since the coupling occurs through chemical bonds, it is called the indirect spin-spin coupling. The splitting patterns and intensity distribution of the multiplets can be predicted using simple rules. The indirect spin-spin coupling is independent of the external field, and the coupling constants *J* are therefore given in Hz. Couplings are observed not only between nuclei of the same species but also between different nuclei (heteronuclear couplings). For our purposes the most important are the H,H and C,H couplings.
- In ^{1}H NMR spectroscopy the signal intensities are also determined for each spectrum, but in routine ^{13}C NMR spectra the intensities cannot be measured.

The relationships between chemical shifts and molecular structure will be examined in detail in Chapter 2, and those between coupling constants and molecular structure in Chapter 3.

1.7 "Other" Nuclides [5, 6]

Up to now we have been concerned almost exclusively with the properties of ^{1}H and ^{13}C nuclei and their NMR spectra. However, it is possible to obtain NMR spectra of nearly all elements, although not always from observations on the isotope with the highest natural abundance, as can be seen from the examples of carbon and oxygen. For reasons connected with the historical development of NMR spectroscopy, nuclei of all species other than ^{1}H are referred to as *heteronuclei*.

The procedures for recording spectra of heteronuclides often differ considerably from those for ^{1}H and ^{13}C, since it is necessary, even for routine measurements, to adjust the experimental conditions to suit the special properties of the nuclei to be observed. For example, the spin–lattice relaxation times for some nuclides, such as ^{15}N and ^{57}Fe, are very long, whereas for others (especially those with an electric quadrupole moment) they are very short. Also the spectra observed for some nuclides contain interfering signals caused by other materials present, for example the glass of the sample tube (^{11}B, ^{29}Si), the spectrometer probe unit (^{27}Al), or the transmitter/receiver coil. For many nuclides the sample temperature and its con-

stancy are important factors; for example, quadrupolar nuclides such as ^{17}O give narrower signals when the temperature is increased. For some nuclides such as ^{195}Pt and ^{59}Co, and also for ^{31}P, the chemical shifts are found to be strongly temperature-dependent, with coefficients that can exceed 1 ppm K^{-1}. Special care is also needed in the choice of a suitable chemical shift standard [1] and of an appropriate spectral range, since often the spectrum may consist of only one peak, and mistakes can easily arise in determining the resonance frequency (for example, where back-folding occurs). In cases where the resonance frequency is low (see Table 1-1) it is often found that the base-line of the spectra is not constant, which causes problems especially in detecting broad signals of insensitive nuclides. In cases such as these it is often necessary to carry out several experiments under different operating conditions to arrive at unambiguous assignments and yield correct spectral data. Nuclides with spin $I = 1/2$ and those with greater spin will be treated separately, as there are fundamental differences between these two cases.

1.7.1 Nuclides with Spin $I = 1/2$

The behavior in a magnetic field of any nucleus with spin $I = 1/2$ is similar to that of ^{1}H and ^{13}C. This group includes ^{3}H, ^{15}N ^{19}F, ^{29}Si, ^{31}P, ^{57}Fe , ^{119}Sn, ^{195}Pt, and many others. Some of these nuclides, such as ^{3}H, ^{19}F, and ^{31}P, are easy to observe (*sensitive* nuclides) , as they have a large magnetogyric ratio γ and a large magnetic moment μ, whereas others, such as ^{15}N and ^{57}Fe, are not so favorable. These insensitive nuclides suffer from the additional disadvantage of low natural abundances (e. g., 0.37 % for ^{15}N and 2.12 % for ^{57}Fe; see Table 1-1). For nuclides such as these the pulsed method of observation is essential, as in the case of ^{13}C. However, this often presents technical problems owing to the fact that the range of chemical shifts for nuclei that differ in their substituents or coordination is usually very large, requiring a correspondingly large spectral width. For example, the range of chemical shifts for ^{195}Pt can be as large as 8000 ppm, and with a magnetic flux density B_0 of 2.35 T (resonance frequency 21.497 MHz for ^{195}Pt or 100 MHz for ^{1}H) this corresponds to a spectral width of about 1.7 x 10^5 Hz!

A few spin 1/2 nuclides, such as ^{57}Fe, have extremely long spin–lattice relaxation times, which requires long delay times between successive pulses during the accumulation of the FID. In such cases one can add paramagnetic compounds such as $Cr(acac)_3$ to reduce the accumulation time to an acceptable value (see Sections 1.5.5 and 1.6.3.2).

1.7.2 Nuclides with Spin $I > 1/2$

By far the majority of heteronuclides belong to the group with $I > 1/2$. A small selection of these are listed in Table 1-1. All such nuclides have an electric quadrupole moment Q, and they usually give broad NMR signals due to the shortening of the relaxation times through the interaction of the quadrupole moment with local electric field gradients (Section 7.3.3). Often this means that one is unable to observe any multiplet splittings due to couplings with other nuclei, or even to resolve chemical shift differences. Exceptions to this are those nuclides that have a relatively small quadrupole moment, such as deuterium, ^{2}H. Other exceptions occur when the quadrupolar nucleus is in a symmetrical environment; a typical example is the ^{14}N resonance of the symmetrical ammonium ion $NH_4^{\oplus}$ (Section 3.7).

For many quadrupolar nuclides, especially the heavier ones, the chemical shifts between non-equivalent nuclei can be extremely large, making it possible to observe separate signals despite the broadness of the resonances (see Section 2.5). For example, the range of chemical shifts for ^{59}Co is about 20 000 ppm, which at $B_0 = 2.35$ T (^{59}Co resonance frequency 23.727 MHz) corresponds to a spectral width of the order of 4×10^5 Hz! However, in addition to the usual technical problems associated with such a large spectral width (Section 1.7.1), there is the difficulty that for very broad signals the pulse duration is of the same order as the relaxation times. In favorable cases, of which ^{59}Co is an example, one can resort to the older CW method of recording (Section 1.4.2), but this is not possible when the natural abundance is so low as to make the pulsed FT method mandatory.

Many nuclides with $I > 1/2$ belong to metals and transition metals that have important functions in biochemistry. In most cases this involves ions in aqueous solutions. Some of the most important ion species are those of the alkali and alkaline earth metals, such as $^{23}Na^{\oplus}$, $^{39}K^{\oplus}$, $^{25}Mg^{2\oplus}$, and $^{43}Ca^{2\oplus}$. Despite the great advances in measurement methods that have occurred, the low detection sensitivity for some of these ions means that one still has to resort to using materials enriched in the relevant isotopes, which is laborious, time-consuming, and costly. This applies particularly to the ions $^{25}Mg^{2\oplus}$ and $^{43}Ca^{2\oplus}$, and also to $^{57}Fe^{2\oplus}$. Another nuclide with a spin greater than 1/2 is ^{17}O ($I = 5/2$), with only 0.038 % natural abundance and a moderately large electric quadrupole moment (Table 1-1), which typically results in line-widths between 20 and 300 Hz.

In conclusion it should be mentioned that for many nuclides of both these classes, including ^{15}N, ^{17}O, ^{25}Mg, and ^{29}Si, the magnetogyric ratio γ is negative (Table 1-1). In terms of the

classical picture this means that the magnetic moment $\boldsymbol{\mu}$ and the angular momentum vector $\boldsymbol{P}$ lie in opposite directions (see Section 1.2). This becomes important especially in experiments that involve the nuclear Overhauser effect (NOE, Section 10.2.2).

Exercises

[1-1] For each of the following compounds name the nuclides for which it is possible to observe NMR signals:
(1) $CF_3COOCH_2CH_3$, (2) $HCON(CH_3)_2$, (3) $P(CH_3)_3$.

[1-2] NMR spectroscopy is a method with comparatively low sensitivity. Why? How do we try to overcome this problem, by approaching it from the instrumental, experimental and chemical standpoints?

[1-3] Name some examples of nuclides with $I = 0$, ½ , 1 and > 1. Why are nuclides with $I \geq 1$ less suitable for NMR spectroscopy?

[1-4] Arrange the following nuclides in the order of their NMR sensitivities: ^{1}H, ^{13}C, ^{15}N, ^{19}F, ^{31}P.

[1-5] What are the quantities that appear in the resonance condition (Eq. 1-12), and what do they mean? What information can one obtain from the resonance condition?

[1-6] Calculate the Larmor frequency of ^{13}C at $B_0 = 11.75$ T.

1.8 Bibliography for Chapter 1

[1] R. K. Harris, E. D.Becker, S. M. Cabral de Menezes, R. Goodfellow and P. Granger. *Nuclear Spin Properties and Conventions for Chemical Shifts (IUPAC Recommendations 2001)*. In: Encyclopedia of Nuclear Magnetic Resonance, Vol. 9. Chichester: John Wiley & Sons, 2002, p. 5ff.

[2] R. R. Ernst and W. A. Anderson, *Rev. Sci. Instrum. 37* (1966) 93.

[3] R. R. Ernst: Nuclear Magnetic Resonance – Fourier Transform Spectroscopy. In: *Angew. Chem. Int. Ed. Engl. 31* (1992) 805.

[4] P. Bigler: *NMR Spectroscopy: Processing Strategies*. 2nd Edition. Weinheim: Wiley-VCH, 2002.

[5] S. Berger, S. Braun, H.-O. Kalinowski: *NMR Spectroscopy of the Non-Metallic Elements*. Chichester: John Wiley & Sons, 1997.

[6] J. Mason (Ed.): *Multinuclear NMR*. New York: Plenum Press, 1987.

Additional and More Advanced Reading

M. H. Levitt: Spin Dynamics – Basics of Nuclear Magnetic Resonance, 2nd Edition. Chichester: John Wiley & Sons, 2008.

R. K. Harris: *Nuclear Magnetic Resonance Spectroscopy. A Physicochemical View.* London: Pitman, 1983.

F. J. M. van de Ven: *Multidimensional NMR in Liquids. Basic Principles and Experimental Methods*. New York: John Wiley & Sons, 1995.

A. E. Derome: *Modern NMR Techniques for Chemistry Research*. Oxford: Pergamon Press, 1987.